Novel Long-chain Neurotoxins from *Bungarus candidus* Distinguish the Two Binding Sites in Muscle-type Nicotinic Acetylcholine Receptors

Yuri N. Utkin[1,2*¶], Ulrich Kuch[3¶], Igor E. Kasheverov[1,4], Dmitry S. Lebedev[1], Ella Cederlund[5], Brian E. Molles[6], Iakov Polyak[1,7], Igor A. Ivanov[1], Nikita A. Prokopev[8], Rustam H. Ziganshin[1], Hans Jornvall[5], Gunvor Alvelius[5], Lawan Chanhome[9], David A. Warrell[10], Dietrich Mebs[11], Tomas Bergman[5], and Victor I. Tsetlin[1]

[1]Shemyakin-Ovchinnikov Institute of Bioorganic Chemistry, Russian Academy of Sciences, Moscow, Russia

[2]The National University of Science and Technology MISIS, Moscow, Russia

[3]Institute of Occupational Medicine, Social Medicine and Environmental Medicine, Goethe University, Frankfurt am Main, Germany

[4]Sechenov First Moscow State Medical University, Institute of Molecular Medicine, Moscow, Russia

[5]Department of Medical Biochemistry and Biophysics, Karolinska Institutet, Stockholm, Sweden

[6]Department of Pharmacology, University of California, San Diego, La Jolla, California, United States of America

[7]School of Chemistry, Cardiff University, Cardiff, United Kingdom

[8]Department of Bioorganic Chemistry, Faculty of Biology, Lomonosov Moscow State University, Moscow, Russia

[9]Queen Saovabha Memorial Institute, Bangkok, Thailand

[10]Nuffield Department of Clinical Medicine, University of Oxford, Oxford, United Kingdom

[11]Institute of Legal Medicine, Goethe University, Frankfurt am Main, Germany

[¶]These authors contributed equally to this work.

Correspondence: Yuri N. Utkin (utkin@ibch.ru; yutkin@yandex.ru)

Abstract

αδ-Bungarotoxins, a novel group of long-chain α-neurotoxins, manifest different affinity to two agonist/competitive antagonist binding sites of muscle-type nicotinic acetylcholine receptors, being more active at the interface of α-δ-subunits. Three isoforms (αδ-BgTx-1-3) were identified in Malayan Krait (*Bungarus candidus*) from Thailand by genomic DNA analysis; two of them (αδ-BgTx-1 and 2) were isolated from its venom. The toxins comprise 73 amino acid residues and 5 disulfide bridges, being homologous to α-bungarotoxin (α-BgTx), a classical blocker of muscle-type and neuronal α7, α8, and α9α10 nicotinic acetylcholine receptors. The toxicity of αδ-BgTx-1 (LD_{50} 0.17–0.28 μg/g mouse, i.p. injection) is essentially as high as that of α-BgTx. In the chick biventer cervicis nerve-muscle preparation, αδ-BgTx-1 completely abolished acetylcholine response, but in contrast to the block by α-BgTx, acetylcholine response was fully reversible by washing. αδ-BgTxs, similar to α-BgTx, bind with high affinity to α7 and muscle-type nicotinic acetylcholine receptors. However, the major difference of αδ-BgTxs from α-BgTx and other naturally-occurring α-neurotoxins is that αδ-BgTxs discriminate the two binding sites in the *Torpedo californica* and mouse muscle nicotinic acetylcholine receptors showing up to two orders of magnitude higher affinity for the α-δ site as compared to α-ε or α-γ binding site interfaces. Molecular modeling and analysis of the literature provided possible explanations for these differences in binding mode; one of the probable reasons being the lower content of positively charged residues in αδ-BgTxs. Thus, αδ-BgTxs are new tools for studies on nicotinic acetylcholine receptors.

Abbreviations list: AChBP, acetylcholine binding protein; BSA, bovine serum albumin; α-BgTx, α-bungarotoxin; αδ-BgTx, αδ-bungarotoxins; α-CTX, α-cobratoxin; hα7, human α7; nAChR, nicotinic acetylcholine receptor

Introduction

Nicotinic acetylcholine receptors (nAChRs) belong to the large family of ligand-gated ion channels and consist of five identical or homologous polypeptide subunits arranged with radial symmetry around a central pore [1-3]. In the muscle type nAChR, two copies of α1 and one each of the β1, δ, and γ subunits (in the embryonic receptor form) or ε subunit (in the adult form) are arranged around that pore in counter-clockwise order α1-γ/ε-α1-δ-β1 [4-5]. The binding sites for agonists and competitive antagonists are located at the interfaces of the α1-δ and α1-γ (or α1-ε) subunits [6]. Full activation of the nAChR requires the simultaneous binding of two agonist molecules, but antagonists can block activation by occupying only one of the two sites [7]. The neuronal α7 type nAChR is composed of five identical α7 subunits and possesses a spatial organization similar to that of the muscle-type receptor [8].

The venoms of snakes of the Elapidae family are rich sources of toxins targeting nicotinic acetylcholine receptors. Structurally, two groups of these toxins are distinguished: "short α-neurotoxins" consisting of 60 - 62 amino acid residues in a single chain that is cross-linked intramolecularly by four disulfide bonds, and "long α-neurotoxins" consisting of 66 - 74 amino acid residues and five disulfide bonds [9]. Collectively, short and long neurotoxins form a part of the "three-fingered" group of snake toxins [10-11]. Their members exhibit a characteristic three-loop topology in which each of the three fingers extends from a core "knuckle" region consisting of four conserved disulfide bonds. Other snake toxins sharing this three-fingered structure include so-called non-conventional or weak toxins [12-13], some of them acting on nAChRs, and functionally quite divergent molecules like cyto-/cardio-toxins, fasciculins (an inhibitor of acetylcholinesterase), toxins blocking muscarinic receptors or calcium channels (calciseptine), and several others whose targets still await identification.

Short and long snake α-neurotoxins like α-bungarotoxin (α-BgTx) [14, 15] from the venom of the Many-banded Krait (*Bungarus multicinctus*) have been used to probe nAChRs for

over 40 years [16]. They continue to be valuable tools in studies of the nAChR structure, function and levels at normal state and in various pathologies (e.g., [10-11, 17]). In recent years, they have been joined by shorter peptides like α-conotoxins [18-20] from cone snail (*Conus* spp.) venoms, waglerins [21] from the venom of the Temple Viper (*Tropidolaemus wagleri*) and azemiopsin of Fea's Viper (*Azemiops feae*) [22] which in contrast to α-BgTx and other frequently used elapid snake neurotoxins were found to discriminate between receptor subtypes, the two binding sites of muscle nAChRs, and the receptors of various animal species [23-25].

Here we report novel snake long-chain neurotoxins, αδ-bungarotoxins (αδ-BgTxs), which have different affinities for the two binding sites of the muscle-type nAChRs, induce reversible block of the nAChR, bind also to the neuronal α7 nAChR, and combine these properties with high toxicity and great structural similarity to the classic receptor probe α-BgTx. The name αδ-bungarotoxins has been selected to highlight this structural similarity as well as their preferential binding at the nAChR α-δ subunit interface.

Materials and Methods

Isolation of αδ-BgTxs

Three different batches of *Bungarus candidus* venom were used in this study: one from snakes from Surat Thani, southern Thailand, kept at the Faculty of Tropical Medicine of Mahidol University, Bangkok (sample A), and two (samples B and C) from southern Thailand snakes kept at the Queen Saovabha Memorial Institute (QSMI), Bangkok. After milking, venom was lyophilized immediately. The separation procedures included gel-filtration, ion-exchange and reversed phase chromatography either essentially as described in [26], or by using a Superdex 75 column (10 × 300 mm, GE Healthcare) for gel-filtration, HEMA BIO 1000CM column (8 × 250 mm, Tessek, Prague, Czech Republic) for ion-exchange chromatography and a Jupiter C18 column (10 × 250 mm, Phenomenex, Torrance, CA, USA) for reversed phase HPLC. Crude *B. candidus* venom (65 mg) was dissolved in 0.65 ml of 0.1 M ammonium acetate buffer (pH 6.2)

and separated on the Superdex 75 column equilibrated with the same buffer at a flow rate of 30 ml/h. The eluting proteins were detected by absorbance at 280 nm. The fractions were pooled (Fig. 1A) and analyzed by mass-spectrometry. Fraction 8 (Fig. 1A), containing toxins with a molecular mass of 8031 and 8143.5 Da, was further separated on the HEMA BIO 1000 CM column using a gradient of 5 to 45 mM ammonium acetate in 100 min at a flow rate of 1.0 ml/min. Fractions obtained (Fig. 1B) were analyzed by mass-spectrometry and separated further on the Phenomenex C_{18} column applying a gradient of 20% to 40 % acetonitrile (v/v, in 60 min) containing 0.1% (v/v) trifluoroacetic acid (TFA), at a flow rate of 2.0 ml/min (Supplementary Figure 1). Purification prior to amino acid sequencing procedures was achieved by RP-HPLC on a BDS-Hypersil-C18 column (125 × 4 mm; Hewlett-Packard, Palo Alto, CA, USA) equilibrated with 0.1% TFA in water, using a linear gradient of 0–80% acetonitrile in 0.1% TFA at a flow rate of 0.5 ml/min over 45 min. Absorbance was monitored at 220 nm.

Molecular mass determination

Venom fractions and isolated toxins were analyzed by HPLC-MS using a Thermo Finnigan LCQ Deca XP mass spectrometer (Thermo Fisher Scientific, Waltham, MA, USA) and a Thermo Accela UPLC system (Thermo Fisher Scientific, Waltham, MA, USA). Detection was performed using UV-VIS DAD and MS (ESI+, 150–2000 units). Peptide mass fingerprinting was performed using Ultraflex III MALDI-TOF/TOF (Bruker Daltonics, Billerica, MA, USA).

Amino acid sequence determination

N-terminal sequence analysis of intact and proteolytically digested toxin samples from venom sample A were performed using a Procise HT sequencer instrument (Applied Biosystems, Foster City, CA, USA) with S-carboxymethylated samples immobilized on PVDF membranes. Carboxymethylation and digestion with Asp-N and Glu-C proteases were performed as described [26]. Digested samples were separated by RP-HPLC using a Vydac C8 column at 0.2 ml/min and detection at 214 nm. N-terminal sequence analysis of the native toxin from venom sample B was

carried out as described [26]. The amino acid sequence of αδ-BgTx-1 has been deposited in the UniProtKB database (primary accession number: A1IVR8).

Cloning and sequence analysis of genomic DNAs encoding αδ-BgTx isoforms

Total DNA was isolated from shed skin material of one of the *B. candidus* from southern Thailand that had been used for venom extraction. PCR, cloning and DNA sequencing were performed as described in [26] using the amplification primers P2 [27], which is based on the 3´-non-coding region of the cobrotoxin and cardiotoxin genes [28], and P5 (Supplementary Table 1), which corresponds to a sequence just upstream of a tandem repeat which in turn is upstream from exon 2 of the α-BgTx (A31) gene [27] (Supplementary Figure 2). The sequences were aligned against the published nucleotide sequences of the α-BgTx (A31) gene and cDNA (accession nos. Y17694 and Y17058, respectively [27]). Sequence similarity was assessed using BLASTN 2.2.8 [29] by comparing the new genomic and their combined coding sequences to the database. Theoretical masses and theoretical isoelectric points (pIs) of polypeptides were calculated using the ExPASy Compute pI/Mw Tool [30]. The nucleotide sequences of the partial genes of the three αδ-BgTx isoforms from Thai *B. candidus* have been deposited in the DDBJ/EMBL/GenBank Nucleotide Sequence Database under the accession numbers AM231681 (partial αδ-Bgt-1 gene for αδ-BgTx-1), AM231682 (partial αδ-Bgt-2 gene for αδ-BgTx-2), and AM231680 (partial αδ-Bgt-3 gene for αδ-BgTx-3).

Toxicity assays

Lethal toxicity was assayed as described [26] in Swiss mice of both sexes weighing 18–20 g. LD_{50} and its confidence limits at 95% probability were calculated by the methods of Reed-Muench [31] and Pizzi [32], respectively. Animal experiments were performed at Queen Saovabha Memorial Institute after approval and under the supervision of the Queen Saovabha Memorial Institute Animal Care and Use Committee (QSMI-ACUC). The experimental procedure was reviewed and approved by the Committee in accordance with Queen Saovabha

Memorial Institute regulations and policies governing the care and use of laboratory animals. The review followed guidelines documented in the "Ethical Principles and Guidelines for the Use of Animals for Scientific Purposes" edited by the National Research Council of Thailand.

Chick biventer cervicis nerve-muscle assay

The neuromuscular blocking activity of αδ-BgTx-1 was compared to that of α-BgTx (A31) as described [33] using the isolated biventer cervicis nerve-muscle preparation from 4–7-day-old chicks. The response of the muscle to acetylcholine (100 μM) was recorded for 60 sec before and after treatment with the toxin fractions. During the test of acetylcholine response, the electrical stimulation was suspended.

Synthesis of radioiodinated αδ-BgTx-1 and α-BgTx

The synthesis of radioactive α-BgTx was carried out essentially as described [34]. For this study, a product with a specific radioactivity of 500 curies/mmol was obtained. α-BgTx (400 pmoles) dissolved in 20 μL of 125 mM sodium phosphate buffer, pH 7.5, was incubated for 10 min at room temperature with a mixture of 100 pmoles of Na[^{125}I] and 300 pmoles of NaI and 4 nmoles of chloramine T. The reaction products were separated by ion-exchange HPLC in a 5 mM sodium-phosphate buffer, pH 7.5, using a gradient of 0.2 M NaCl (2–62% for 30 min) on a TSKgel CM-5PW column (75 × 7.5 mm) at a flow rate of 0.5 mL/min. Detection was carried out at 226 nm and the iodinated products were collected in 0.5 min fractions. Aliquots of all fractions were counted on a Wizard 1470 Automatic Gamma Counter (Perkin Elmer, Shelton, CT, USA). The mono-iodinated [^{125}I]α-BgTx derivative (with approximate specific radioactivity of 500 Ci/mmol) was collected and kept not longer than 1 month at 4 °C in a 50 mM Tris-HC1 buffer, pH 7.5, containing 0.1 mg/ml BSA.

Radio-iodinated αδ-BgTx-1 was prepared according to the same protocol as above, but using 280 pmoles of the toxin, 70 pmoles of Na[^{125}I], 210 pmoles of NaI and 2.8 nmoles of chloramine T, and applying a different gradient (5–60% for 60 min) with the same column and

solutions to separate the iodination products. Mono-iodinated [^{125}I]αδ-BgTx-1 and α-BgTx derivatives were used in parallel experiments of radioligand assays on muscle-type nAChR from the electric organ of the *Torpedo californica* ray and human α7 (hα7) nAChR expressed in GH4C1 cells.

Receptor binding assays

Four types of nAChR were examined: the adult (α1β1δε) and embryonic form (α1β1δγ) mouse muscle nAChRs, the α1β1γδ muscle-type nAChR from the electric organ of *T. californica*, and the neuronal hα7 nAChR expressed in the GH4C1 cell line. For competition binding assays using mouse muscle nAChRs, cloned cDNAs for mouse α1, β1, δ, and ε or γ nAChR subunits were sub-cloned into the CMV promotor-based mammalian expression vector pRBG4 [35] at EcoRI sites. The individual subunit cDNAs of the nAChR are present on separate plasmids. HEK293 cells were transfected using the calcium phosphate precipitation method [36]. The medium was changed 12–16 h later and the experiments were performed 1-2 days after the medium change. GH4C1 cells transfected with hα7 nAChR cDNA were a gift of the Eli-Lilly Co. (London, UK). Muscle-type nAChR-enriched membranes from the electric organs of *T. californica* were kindly provided by Prof. F. Hucho (Free University of Berlin, Germany). The binding assays on mouse muscle nAChRs were performed using αδ-BgTxs, a commercial sample of unlabeled α-BgTx (Sigma-Aldrich, St. Louis, MO, USA), α-BgTx (A31) isolated from Javan *B. candidus* venom [26], [^{125}I]α-BgTx (New England Nuclear, Boston, MA, USA), or α-conotoxin MI (American Peptide Co., Sunnyvale, CA, USA) which had been radioiodinated as described [37]. The binding assays on neuronal hα7 and *T. californica* nAChRs were performed using αδ-BgTxs, and with α-BgTx (A31) isolated from Vietnamese *B. multicinctus* venom obtained as described [38].

Estimation of αδ-BgTx-1 binding to mouse muscle nAChRs

To dissociate the transfected cells from plates, the culture medium was removed, and the cells were gently agitated with 5 ml PBS (pH 7.4) containing 5 mM EDTA. The dissociated cell suspension was centrifuged at 1000 *g* for 1 min and re-suspended to a final concentration of 40-100 pM α-BgTx binding sites in high K+ Ringer's buffer (140 mM KCl, 5.4 mM NaCl, 1.8 mM $CaCl_2$, 1.2 mM $MgCl_2$, 25 mM HEPES, and 30 mg/l bovine serum albumin [BSA]). Aliquots of intact dissociated cells were incubated overnight with the test toxin at room temperature to ensure equilibrium was reached between toxin and receptor. [^{125}I]α-BgTx was added to a final concentration of 5 nM and allowed to incubate 30 min with the receptor until 30–50% of the available binding sites were occupied [36, 37, 39]. The fraction of the nAChR binding sites occupied by αδ-BgTx-1 was determined by calculating the reduction of the initial association rate of [^{125}I]α-BgTx observed in the presence of each concentration of competing toxin (kon_{obs}) compared to the maximum association rate in the absence of the competing ligand (kon_{max}). The total number of sites was determined by incubation with 20 nM [^{125}I]α-BgTx for 1 h.

Nonspecific binding was determined by incubating the cells with 10 mM carbachol or 10 μM unlabeled α-BgTx before adding [^{125}I]α-BgTx; comparable values of non-specific binding were obtained for both carbachol and α-BgTx. In a separate series of assays, 30 nM α-conotoxin MI was added to the assay mixture after incubation with αδ-BgTx-1 and before adding [^{125}I]α-BgTx. This concentration of α-conotoxin MI will occupy ~98% of the available αδ subunit interface sites and <10% and <1% of the αε and αγ interface bindings sites, respectively [37]. Transformed data were fit to the one site or two site Hill equation using Prism 3.0 (Graphpad).

Estimation of αδ-BgTx binding to *Torpedo californica* muscle-type and human neuronal α7 nAChRs

For competition binding assays, suspensions of nAChR-rich membranes from *T. californica* electric organ (1.25 nM α-bungarotoxin binding sites) in 20 mM Tris-HCl buffer pH 8.0 containing 1 mg/ml BSA (binding buffer) or hα7 nAChR transfected GH_4C_1 cells (0.9 nM α-

bungarotoxin binding sites) in binding buffer were incubated for 1.5 h at room temperature with various amounts of the different αδ-BgTxs, followed by an additional 30 min incubation with 1 nM [^{125}I]α-BgTx. Nonspecific binding was determined by preliminary incubation of the preparations with 20 μM α-cobratoxin. The membrane and cell suspensions were applied to glass GF/C filters (Whatman, Maidstone, UK) presoaked in 0.25% polyethylenimine, and unbound radioactivity was removed from the filter by washing (3 × 3 ml) with 20 mM Tris-HCl buffer, pH 8.0, containing 0.1 mg/ml BSA (washing buffer). The bound radioactivity was determined using a Wizard 1470 Automatic Gamma Counter. The binding results were analyzed using ORIGIN 7.5 (OriginLab Corporation, Northampton, MA, USA) fitting to one site or two site dose-response competition curves.

The equilibrium saturation binding of the [^{125}I]αδ-BgTx-1 with the *T. californica* nAChR (1.25 nM α-bungarotoxin binding sites) or hα7 nAChR in GH4C1 cells (0.9 nM α-bungarotoxin binding sites) was carried out in 50 μL of binding buffer at room temperature. Various concentrations of the radioligand (0.02–1.25 nM) were incubated with the targets for 1 hr. Non-specific binding was determined in the presence of 10 μM of α-cobratoxin (1 h pre-incubation). The filtration on GF/C filters was performed as mentioned above. The equilibrium binding data were fitted using ORIGIN 7.5 to a one site model according to the Equation: $B(x) = B_{max}/(1 + K_d/x)$, where B(x) is the radioligand specifically bound at free concentration x (determined by subtracting the amount of bound and adsorbed radioligand from the total amount added to the incubation mixture), B_{max} is the maximal specific bound radioligand, and K_d is the dissociation constant.

Estimation of dissociation kinetics by radioligand analysis

To evaluate the dissociation kinetics of [^{125}I]αδ-BgTx-1 and [^{125}I]α-BgTx from the complex with the *T. californica* nAChR or hα7 nAChR, binding of the 0.3 nM radioligands was allowed to reach equilibrium (1.5 h incubation) in binding buffer at room temperature, after

which a saturating concentration of α-cobratoxin (10 μM) was added to prevent any re-association of the radioligands to the receptors. The reactions were terminated by rapid filtration on the GF/C filters as mentioned above for different time intervals (2 to 120 min). To calculate k_{off} values, the experimental data were fitted to an exponential equation:

$B_p = 100 \times$ (− ×), where B_p is the percentage of the binding complex, t is time (min).

In the case of [^{125}I]αδ-BgTx-1 dissociation from the *T. californica* nAChR the best fit was achieved with a biexponential equation: $B_p = a1 \times (- 1 \times) + a2 \times (- 2 \times)$,

where a1 + a2 = 100%.

Electrophysiological assays on *Xenopus* oocytes

Electrophysiological assays on *Xenopus laevis* oocytes were performed as described [40]. Various concentrations of αδ-BgTx-1 were first applied to an oocyte for 5 min, followed by adding the agonist ACh (30 μM, which is equal to the EC_{100} on muscle type nAChR and the EC_{10} on α3β2 nAChR). To test the reversibility of the nAChR block produced by αδ-BgTx-1, the receptor was incubated with 0.112 mg/ml αδ-BgTx-1 for 10 min. Then the oocytes were washed with bath buffer (0.4 ml/min) and the response to 30 μM ACh was measured every 5 min.

Molecular modeling of αδ-BgTx-1 and docking simulations

The structure of α-BgTx was taken from the crystal structure of its complex with the extracellular domain of the nAChR α1 subunit [41]. A model of the structure of αδ-BgTx-1 was built with the Modeller 8v1 package [42] using the α-BgTx structures as a template. The model of the acetylcholine binding protein (AChBP) of *Lymnaea stagnalis* was taken from the α-cobratoxin-AChBP crystal structure ([43]; PDB 1YI5). Extracellular domains of the α and γ subunits of the *T. californica* nAChR were built with the Modeller 8v1 package using the structure of the *T. marmorata* nAChR ([44]; PDB 2BG9) as a template. The position of the C-

loop in the nAChR model was adopted from the α-cobratoxin-AChBP crystal structure [43]. Docking simulations were performed using the programme HEX 4.5 (http://www.csd.abdn.ac.uk/hex/) [45].

Results

Isolation of αδ-BgTxs

Three different batches of *B. candidus* venom from southern Thailand were used in this study for the isolation of αδ-BgTxs. In one purification scheme, the crude venom was separated first by gel-filtration on a Superdex 75 column (Fig. 1A). Twelve fractions were collected and analyzed by mass-spectrometry. Fraction 8, containing toxins with molecular masses of 8031 and 8143.5 Da, was further separated by ion exchange chromatography (Fig. 1B). Likewise, the seven fractions obtained were analyzed by mass-spectrometry. The MS-spectra of fractions 3 and 4 were identical showing one major peak corresponding to a molecular mass of 8143.5 Da. MS-spectra of fractions 6 and 7 were also identical exhibiting a molecular mass of 8031 Da. The fractions 3, 4, 6 and 7 were further purified by reversed phase HPLC (Supplementary Figure 1) and were used for further studies. Fractions 3 and 4 showed very similar profiles with one predominant peak of a molecular mass of 8143.5 Da. One main peak was seen in the profiles of fractions 6 and 7 with a molecular mass of 8031 Da. Peptide mass fingerprinting confirmed the identity of proteins in fraction 3 and 4 as well as in fractions 6 and 7, respectively.

To obtain more material for the study, two other batches of crude venom were fractionated essentially as described [26] using gel-filtration on Sephadex G-75, ion-exchange chromatography on SP-Sephadex C-25 and Resource S columns, and finally by RP-HPLC on a BDS-Hypersil-C18 column.

Genomic DNA sequence analysis

PCR amplification using genomic DNA from *B. candidus* and the primers P2 and P5 provided PCR fragments which migrated as a single band in agarose gel electrophoresis and

were estimated to be ~1 kb. The DNA fragments were subcloned and clones were selected for nucleotide sequencing of both strands. Three unique genomic DNAs of 910, 930 and 934 bp were unequivocally constructed from the nucleotide sequences. They were composed of sequences that correspond to the complete toxin-coding regions of the two previously reported genomic DNAs for α-BgTx A31 and V31, which consist of 2924 and 2925 bp [27]. Alignment of the cDNA sequence and the gene for α-BgTx (A31) with the genomic DNAs obtained from *B. candidus* allowed the assignment of intron/exon boundaries, which are virtually identical to those of the α-BgTx (A31) genes of *B. multicinctus* from Taiwan [27] and *B. candidus* from Java [26]. They confirm the common gene organization of elapid snake cardiotoxins, short neurotoxins, and long neurotoxins, i.e., three exons separated by two introns inserted into similar positions in the coding regions [27, 28, 46-48; Supplementary Figure 2]. Compared to α-BgTx (A31) [26, 27], the three αδ-BgTx encoding genomic DNAs from Thai *B. candidus* include a much larger partial intron 1 region (138 bp) that has a 102 bp insertion with high (97%) similarity to an upstream intron 1 sequence from the α-BgTx A31 gene of Taiwanese *B. multicinctus* but lacks a tandem repeat that is inserted in close proximity of the 3'-splice acceptor site of the α-BgTx genes (positions 1886 to 2089 in the A31 variant [27]). They also lack an (AT)9 dinucleotide repeat upstream from the 3'-splice acceptor site, which is present in the α-BgTx A31 genes of both *B. multicinctus* from Taiwan and *B. candidus* from Java. Both exon 2 (with a one-codon deletion) and intron 2 (consisting of 534 vs. 537–539 bp) of the three αδ-BgTx encoding genomic DNAs are shorter than those of the α-BgTx A31 genes. The 5'-splice donor sequence of exon 2 of the αδ-BgTx DNAs (ATGGT) also differs from that of the α-BgTx A31 and V31 genes (ATTCT) [26, 27]. The first exon of the three partial αδ-BgTx genes encodes a part of the signal peptide of α-BgTx (Gly, Tyr, Thr) and the 31 N-terminal amino acids of the mature toxins (32 in α-BgTx; Fig. 2). Their second exon region is highly similar to that of exon 3 of the α-BgTx genes and encodes the 42 C-terminal amino acids of the mature toxins and a short

fragment of the subsequent 3'-non-coding region. The three αδ-BgTx DNAs encode the mature αδ-BgTx polypeptide sequence as determined by amino acid sequencing (αδ-BgTx-1) and two additional isoforms (αδ-BgTx-2 and αδ-BgTx-3) that differ from αδ-BgTx-1 in having Val40 (like α-BgTx) and Asp74 instead of Gly74 as in αδ-BgTx-1 and α-BgTx. Ile9 and Ile31 in αδ-BgTx-2 differentiate it from αδ-BgTx-1, αδ-BgTx-3 and α-BgTx (Fig. 2; Supplementary Figures 3 and 4).

Mass spectrometry analysis and amino acid sequences

The toxins in fraction 3, 4, 6 and 7 were subjected to ESI-MS analysis (Fig. 3). The MS-spectra of the proteins in fraction 6 and 7 were similar; they showed a main component with a mass of 8030.4 Da and four minor components with masses of 8046.4, 8069.5, 8094.3 and 7973.5 Da (Fig. 3). The main component corresponds to αδ-BgTx-1, that of 8046.4 Da to the toxin with oxidized methionine, and those with higher molecular masses may correspond to Na+ and/or K+ adducts of the toxin and its oxidized products. The signal at 7973.5 Da may result from partial cleavage of C-terminal glycine. The spectra of the products from fraction 3 and 4 were also similar and showed a main component with a mass of 8143.5 Da and three minor components with masses of 8159.2, 8172.7 and 8197.4 Da (Fig. 3). The main component corresponds to αδ-BgTx-2, that of 8159.2 Da to a methionine oxidized toxin and those with higher molecular masses to Na+ and/or K+ adducts.

N-terminal sequence analysis of intact αδ-BgTx-1 was successful up to residue 32 (Fig. 2). To determine the complete sequence, the carboxymethylated preparation of αδ-BgTx-1 was digested using Asp-N and Glu-C specific proteases, and the resulting fragments were isolated by RP-HPLC for subsequent Edman degradation. Overlapping sequences accounting for 72 of the 73 residues in the αδ-BgTx-1 polypeptide were obtained (Fig. 2). The identity of the missing residue (position 52) was established by comparing the theoretical mass based on the results of Edman degradation and the polypeptide total mass determined by ESI-MS (above); it revealed a

Pro-residue in position 52 (Fig. 2). The result from the amino acid sequence analysis of the αδ-BgTx-1 preparation agrees completely with the results of the DNA sequence analysis. Sequence comparison between αδ-BgTx-1 and α-BgTx (A31) reveals only ten substitutions (I1L, V2L, H4Y, T5K, T8P, S12N, V14E, R25T, F32W, V40I) and one deletion (Ala7), respectively. In total, the primary structure differences between α-BgTx A31 and αδ-BgTx-1 comprise four charge-modifying mutations (basic in α-BgTx → hydrophobic in αδ-BgTx H4Y; polar → basic T5K; hydrophobic → acidic V14E; basic → polar R25T) resulting in one net (cation → anion) charge reversal (Fig. 2).

The amino acid sequence of αδ-BgTx-2 was confirmed by peptide mass fingerprinting of reduced and carbamidomethylated toxins from fractions 3 and 4 after digestion with trypsin. The amino acid sequence of the tryptic peptides analyzed by MALDI mass spectrometry (Table 1) confirmed the identity of the toxins in the two fractions. With exception of short peptides in the middle of the toxin sequence and at the C-terminal, which are hardly detected by MALDI-MS, the deduced amino acid sequence of αδ-BgTx-2 was almost completely covered by that of the tryptic peptides, suggesting that the isolated toxins represent αδ-BgTx-1 and αδ-BgTx-2.

Toxicity

The LD_{50} determined by i.p. injection for two different batches of αδ-BgTx-1 isolated as described in [26] was in the range from 0.17 to 0.28 μg/g. The LD_{50} of α-BgTx (A31) isolated from *B. candidus* venom was estimated to be 0.13 μg/g. The symptoms produced in mice by αδ-BgTx-1, such as flaccid paralysis and respiratory distress, were similar to those evoked by injection of α-BgTx. αδ-BgTx-1 caused death in a dose-dependent manner as is typical for α-BgTx [49]. Death occurred mostly within 2 to 4 h.

Neuromuscular blocking activity of αδ-BgTx-1

In the chick biventer cervicis nerve-muscle preparation, both αδ-BgTx-1 and α-BgTx (A31) produced complete neuromuscular block at all concentrations tested: 12.5 nM – 1.25 μM

and 3.76 nM – 125 nM, respectively. The time to complete neuromuscular block was similar for αδ-BgTx-1 and α-BgTx at concentrations of 37.6 and 125 nM, but was shorter for α-BgTx at 12.5 nM (Table 2). Considering the postsynaptic mode of action at the motor endplate, the response to acetylcholine was completely abolished when the neuromuscular transmission was blocked by either toxin at all concentrations. However, in marked contrast to the block induced by α-BgTx, acetylcholine response was completely reversible by washing in the case of αδ-BgTx-1 (Table 2).

Binding of αδ-BgTx-1 to the α1β1δε and α1β1δγ mouse muscle nAChRs

αδ-BgTx-1 showed about 100 to 300 times higher affinity to one of the two ligand binding sites of the adult (α1β1δε) and embryonic form (α1β1δγ) of mouse muscle nAChRs than α-BgTx (Fig. 4). The calculations using a two sites competition model resulted in IC_{50} values of 0.0212 ± 0.0032 and 0.115 ± 0.016 nM for high affinity sites on α1β1δε and α1β1δγ receptors, respectively. The IC_{50} values for low affinity sites were almost the same for both receptor types: 20.3 ± 1.2 and 21.8 ± 3.3 nM for α1β1δε and α1β1δγ nAChRs, respectively. A competitive binding of αδ-BgTx-1 in the absence and presence of α-conotoxin MI, which selectively binds to the αδ-binding site of the receptor, demonstrated that the binding site selectivity of αδ-BgTx-1 is directed to the αδ-subunit interface of the mouse muscle nAChR (Fig. 4). In the presence of α-conotoxin MI, competition of αδ-BgTx-1 only for the low affinity site was observed. The calculated IC_{50} values were 15.7 ± 1.2 and 2.54 ± 0.32 nM for α1β1δε and α1β1δγ receptors, respectively. The IC_{50} for the adult receptor was comparable to that of the low affinity site determined in the absence of conotoxin, while the similarity was less pronounced for the embryonic receptor.

Binding of αδ-BgTxs to human neuronal α7 and *Torpedo californica* nAChRs

The capability of αδ-BgTxs to interact with nAChRs was studied by competitive radioligand assay using muscle-type nAChR from the *T. californica* electric organ, the neuronal

hα7 nAChR, heterologously expressed in GH4C1 cells, and [^{125}I]α-BgTx (A31), which bound to these receptors with K_D values of 0.13 ± 0.04 nM and 0.27 ± 0.03 nM, respectively.

On the *T. californica* nAChR, the IC_{50} for α-BgTx was 1.23 ± 0.06 nM, while it was 11.4 ± 1.8 nM for αδ-BgTx-1 and 77 ± 9 nM for αδ-BgTx-2 using a one site competition model (Fig. 5A). However, the calculations using a two sites competition model corresponded more precisely to the data obtained (Fig. 5A), resulting in IC_{50} values of 2.0 ± 1.0 and 34 ± 12 nM for αδ-BgTx-1, and of 15 ± 5 and 210 ± 50 nM for αδ-BgTx-2. The respective K_i values calculated using the Cheng and Prusoff equation [50] and Hill coefficients (nH) are presented in Table 3.

IC_{50} values calculated using a one site competition model for the neuronal hα7 nAChR were 1.18 ± 0.05 nM for αδ-BgTx-1, 5.2 ± 0.6 nM for αδ-BgTx-2 and 0.87 ± 0.11 for α-BgTx (Fig. 5B). The respective K_i values and Hill coefficients are provided in Table 3. On the α7 nAChR, αδ-BgTxs have affinities and nH values comparable to those of α-BgTx. However, on the muscle-type receptor there is a noticeable difference in binding parameters between αδ-BgTxs and α-BgTx. High nH values for ligand binding to nAChRs were observed earlier by our [51] and other research groups [52] and might be explained by the limitations of the Hill equation, for example, because of the assumption that ligand molecules bind to a receptor simultaneously.

To obtain parameters of direct interaction of αδ-BgTx-1 with these two targets, its radioiodinated derivative with 500 Ci/mmol was used. Saturating *T. californica* electric organ membranes (Fig. 6A) and hα7 receptor of GH4C1 cells (Fig. 6B) with [^{125}I]αδ-BgTx-1 resulted in the following binding parameters: for α1β1δγ nAChR - K_d = 0.34 ± 0.03 nM and B_{max} = 0.66 ± 0.02 nM; for the hα7 receptor - and K_d = 0.52 ± 0.05 nM and B_{max} = 1.12 ± 0.06 nM.

The dissociation constants are very close to the corresponding K_i values (see Table 3). It should be noted that in a direct radioligand assay using a radioligand ([^{125}I]αδ-BgTx-1) with a specific radioactivity of 500 Ci/mmol, only a high-affinity binding site on the α1β1δγ nAChR can be detected. Kinetics of the αδ-BgTx-1 dissociation from the complex with nAChRs

compared to that of α-BgTx (Fig. 6) indicate that αδ-BgTx-1 dissociated much faster than α-BgTx from the complex with *Torpedo* nAChR (Fig. 6C), while the release rate from the hα7 nAChR complex was similar for both toxins (Fig. 6D). The kinetics of the αδ-BgTx-1 dissociation from *Torpedo* nAChR is better described by a two sites model with k_{off} of 0.10 ± 0.04 and 0.009 ± 0.001 min^{-1}. For α-BgTx, this value was equal to 0.0017 ± 0.0006 min^{-1}. The k_{off} values for hα7 nAChR were 0.0031 ± 0.0003 and 0.0022 ± 0.0006 min^{-1} for α-BgTx and αδ-BgTx-1, respectively.

Electrophysiological assays

As in the binding experiments on α7 nAChR, αδ-BgTx-1 produced effects similar to those of α-BgTx (Table 3), its activity was not tested on this receptor subtype in electrophysiological experiments. Instead, mouse muscle and human neuronal α3β2 nAChRs that had been heterologously expressed in *Xenopus* oocytes were assayed. It was found that a 10 min treatment of oocytes with αδ-BgTx-1 resulted in a decrease of the ACh-induced current (Fig. 7 A and B). Peak response suppression was dependent on the αδ-BgTx-1 concentration (Fig 7 A and B). The IC_{50} values were 30 ± 9.8 nM (n = 5) for muscle type and 2.9 ± 0.48 (n = 4) μM for neuronal α3β2 receptors. At a concentration of 270 μM α-BgTx only insignificantly (less than 30%) inhibited α3β2 nAChR.

To test the reversibility of αδ-BgTx-1 action, oocytes expressing mouse muscle nAChRs and neuronal α3β2 nAChRs were incubated with 15.2 μM αδ-BgTx-1 for 10 min. The toxin was then washed out at a flow rate of 0.4 ml/min and the receptor response to 30 mM ACh was determined every 5 min (Fig. 7 C and D).

The α3β2 nAChR recovered very fast, and full recovery was observed after 10 min washing. The recovery of the muscle type receptor was slower and reached only about 50% after 30 min washing. These results demonstrate that in contrast to α-BgTx, the action of αδ-BgTx-1 is easily reversible.

Molecular modeling of αδ-BgTx-1 and docking simulations

Comparison of the models of free α-BgTx and αδ-BgTx-1 shows a slight difference in the spatial structure of the first loop where αδ-BgTx-1 exhibits a sharper β-turn due to its deletion of Ala7 and the P8T substitution (Fig. 8). Docking simulations of α-BgTx and αδ-BgTx-1 to AChBP, and to the interface of the α and γ subunits at the extracellular domain of the *Torpedo* nAChR, resulted in complexes that were very similar to the published α-CTX-AChBP crystal structure [43]. The first loop of the toxin contacted the C-loop of the main (positive) side of the binding pocket, and α-BgTx seemed to create more contacts in this area than αδ-BgTx-1.

According to the αδ-BgTx-1 homology model and its template α-BgTx in their complexes with the ligand-binding domain of the α1 subunit (see Fig. 8), as shown in the X-ray structure of α-BgTx bound to the extracellular domain of the α subunit [41], the only structural difference between the two toxins that may result in different affinities, is the shortening of loop I leading to a smaller number of contacts with the carbohydrate chain. The receptor C-loop is too far to form direct contacts with this part of the toxin loop I. The F32W substitution in loop II may push the Arg36 side chain closer to the receptor's loop C residues. However, the rigid homology modeling performed does not allow us to speculate on possible effects of this substitution on the toxin's affinity.

Discussion

Following a general purification scheme with three chromatographic steps, new toxins called αδ-bungarotoxins were isolated from *B. candidus* venom. Interestingly, two isoforms differing in ion-exchange chromatography retention times were observed for both αδ-BgTx-1 and αδ-BgTx-2 (Fig. 1). These isoforms have identical mass spectra and amino acid sequences as confirmed by peptide mass fingerprinting. This finding may be explained by the presence of interconvertible conformers of toxin molecules. A similar behaviour was observed for α-BgTx under HPLC conditions [53]. Mass spectrometry analysis of the isolated toxins revealed some

additional masses which were assigned to methionine oxidation and ion adducts. Methionine oxidation is a very common modification of animal toxins. For example, a toxin with completely oxidized methionine residue was purified from scorpion venom [54], and a similarly modified phospholipase A_2 was isolated from snake venom [55]. Toxin derivatives with oxidized methionine are not always easily separated from original toxins. For example, a 37-residue scorpion toxin (kaliotoxin) was not resolved from its oxidized derivative under isocratic HPLC conditions [56]. Thus, it is possible that αδ-BgTx derivatives with oxidized methionine are not separated from unmodified toxins. In the mass spectrum of αδ-BgTx-1, a signal corresponding to the mass of 7973.5 Da was observed and assigned to a toxin derivative without C-terminal glycine residue. The removal of a small uncharged glycine residue may not strongly change the chromatographic properties of αδ-BgTx-1 resulting in co-elution of such a shortened analogue with the unmodified toxin. In some animal toxins C-terminal glycine undergoes oxidative cleavage with amidation of the C-terminus. However, in snake venoms only one C-amidated toxin (α-elapitoxin-Dpp2d) has been found so far [57]. Overall, C-terminal glycine is not common in snake neurotoxins. Among three-finger neurotoxins isolated from snake venoms we were able to find only one more toxin with a C-terminal glycine in addition to αδ-BgTx-1 and α-BgTx, α-elapitoxin Dv2a from the venom of the Western Green Mamba (*Dendroaspis viridis*). Interestingly, a variant of this toxin that lacks a C-terminal glycine was isolated from the mamba venom along with the original toxin [58].

The three novel nicotinic receptor antagonists (αδ-BgTxs) from the venom of *B. candidus* constitute a novel subgroup of snake long-chain α-neurotoxins with high similarity to the classic receptor probe α-BgTx. In spite of the paucity of structural differences between α-BgTx and αδ-BgTx-1, there are dramatic functional differences between them: binding-site selectivity at the mouse muscle and *T. californica* nAChRs, reversibility in the chick biventer cervicis nerve-muscle preparation, and some differences in their action on mouse muscle and neuronal α3β2

nAChRs. These findings are entirely new for the group of snake long-chain neurotoxins rendering αδ-BgTxs promising natural tools for probing nAChRs of various species and subtypes.

Compared to the LD_{50} calculated here for α-BgTx and previously reported values (e.g., 0.15 μg/g [15] and 0.23 [0.17-0.30] μg/g [26], both by i.p. injection), the lethal toxicity of the two αδ-BgTx-1 preparations for mice is only marginally lower. Their high toxicity, along with the fact that αδ-BgTx-1 and αδ-BgTx-2 are the major polypeptide toxins of Thai *B. candidus* venom (Fig. 1), suggests that αδ-BgTxs assume an important biological role for subduing the prey of these snakes. α-Neurotoxins utilize a common binding core consisting of positively charged and aromatic residues to establish contacts with key invariant residues on the nAChR. Moreover, each toxin uses other residues to recognize and interact with subtype-specific receptor residues. Data from mutagenesis studies, pairwise mutagenesis and structural data on α-BgTx binding to α1- or α7-fragments [59-61] or to combinatorial peptides [62-64], X-ray structure data of the α-CTX-AChBP complex [43] and of the crystal structure of α-BgTx bound to the extracellular domains of the mouse nAChR α1 subunit [41], to neuronal α9 [65] or to the chimera of AChBP and to the α7 domain [66], provide a conceptual framework for inferences regarding some of the differences between αδ-BgTx-1 and α-BgTx. For example, based on the localization of some toxin sites remote from those of the receptor, it can be assumed from the models that the four charge-modifying mutations - three of them (H4Y, T5K, V14E) in loop I of the toxin and the fourth (R25T) in loop II - as well as the hydrophobic↔hydrophobic substitutions I1L and V2L or the polar↔polar substitution S12N have no effect on the activity.

The functional significance of the multiple cationic and aromatic residues of α-neurotoxins, in particular of lysines, arginines, tryptophans, and phenylalanines of loop II, has been independently verified by mutagenesis studies on the short-chain neurotoxin erabutoxin a from the venom of the sea snake *Laticauda semifasciata* [67], on the binding-site selective

mutant of the short-chain neurotoxin *Nmm*I from the spitting cobra *Naja mossambica* [39], and by structural studies of α-BgTx complexes with nAChR fragments [61]. The most critical residue of the short-chain neurotoxins is an invariant Arg33 located at the very tip of loop II [67] which engages in electrostatic interactions with multiple electronegative residues of the receptor [39]. In α-BgTx, the invariant residue Arg36 together with Lys38 forms a cationic cluster at the tip of loop II of both αδ-BgTx-1 and α-BgTx (Figs. 2, 8). In this important region of αδ-BgTx-1 and α-BgTx, there are only three substitutions, namely R25T, V40I, which are relatively close to the tip of loop II, and F32W, which is also located at the tip (Figs. 2, 8). The R25T substitution is constant in all three isoforms of αδ-BgTxs and reduces the cationic charge of these toxins in a region of α-neurotoxins that is known to be critical for receptor binding [39, 59-60]. Val40 of α-BgTx is known to interact with residues Y187 and E188 of the neuronal α7 nAChR [61] and with residue S191 in the extracellular domain of the mouse α1 nAChR [41]. However, it seems doubtful that the mere introduction of an additional methyl group by the V40I substitution (which is present only in αδ-BgTx-1; Fig. 2) would have significant effects on these interactions. αδ-BgTx-2, being less active than αδ-BgTx-1, contains a Val-residue at this position. The third substitution in loop II (F32W) - although retaining the aromatic character at this position - introduces a more bulky residue to an exposed site at the tip of loop II, changing the three-dimensional configuration at the tip of the loop due to the differing functional groups of these residues (Fig. 8) which in turn may result in an alteration of toxin selectivity.

According to the structure of the complex consisting of the extracellular domain of the nAChR subunit α1 with α-BgTx [41], the tip of α-BgTx loop II possesses a helix-like conformation resulting in the same orientation of the Arg36 and Phe32 side-chains which are directed to the main side of the binding pocket: Phe32 serves as part of a "hydrophobic box" and Arg36 protrudes into the box, resulting in multiple π-cation interactions with the receptor's aromatic residues.

Another remarkable structural difference shared by all three αδ-BgTxs, namely the deletion of Ala7 in the α-BgTx sequence (Fig. 2), is likely to be involved in the divergent functional properties of αδ-BgTx-1. Located at the tip of loop I, this residue of α-BgTx, as well as the Thr6, Thr8 and Ser9 residues, make numerous polar contacts with the sugar moiety of the α1 subunit [41]. In addition, the deletion of the Ala-residue leads to a reduction of the number of amino acids that are exposed in the direction of the receptor. According to published structures and docking data, this may affect the function of neighbouring residues and explain their different affinities to nAChRs [68]. Among long-chain neurotoxins, Thr8 is highly conserved and was found to interact with residues W187, K185, and L199 of the α1 subunit of the *T. californica* nAChR [60]. The substitution of this functionally significant residue by hydrophobic proline (T8P) in all three αδ-BgTx isotoxins is remarkable and may play an important role in the divergent binding properties of αδ-BgTx-1.

Both short- and long-chain α-neurotoxins in general and α-BgTx in particular [69] do not distinguish between binding sites in the mouse muscle nAChR. However, mutation studies on the recombinant short neurotoxin *Nmm*I from *N. mossambica* venom showed that removal of a positive charge at conserved residues in loop II of the toxin (K27E or R33E) led to an overall decrease in receptor affinity, while introducing other residues resulted in mutants that recognized with high affinity the αδ site [39]. Thus, the R25T positive charge removal in loop II of αδ-BgTxs may be of similar significance for distinguishing the two binding sites in the muscle-type nAChR. As the nAChR δ-subunit has a larger F-loop (residues 163-177) than the γ-subunit (residues 165-171), this may slightly "push" αδ-BgTx towards the complementary side of the binding pocket, rendering its position more like that of α-BgTx. This may increase the number of interactions between its first loop, the nAChR C-loop and the carbohydrate chain, which may contribute to the increased affinity of the toxin to the αδ binding site. Previously, it has been found that the inhibition of the muscle (α1β1γδ) nAChR by the non-conventional toxin candoxin

from *B. candidus* venom was characterized by different affinities for the two distinct binding sites on the receptor [70]. Some explanations have been suggested, however, further studies are necessary to understand these differences in affinity.

The results of the present study show that αδ-BgTx-2 is about one order of magnitude less active than αδ-BgTx-1 in receptor competition with α-BgTx. Differences in the amino acid sequence of the two toxins include replacement of S9, A31, I40 and G74 in αδ-BgTx-1 by I9, I31, V40 and N74 in αδ-BgTx-2, respectively. The changes to more bulky residues at positions 9 and 31 in αδ-BgTx-2 may disturb its interactions within the receptor binding site. A decrease in the net positive charge by replacing G74 with Asp may further affect toxin-receptor interactions.

In contrast to α-BgTx, blocking of the nicotinic receptor by αδ-BgTx-1 in the isolated chick biventer cervicis nerve-muscle preparation was completely reversible by washing. The same effect was also observed in electrophysiological experiments using mouse muscle and neuronal α3β2 nAChRs as well as in radioligand experiments on *Torpedo* nAChR. Similar effects were reported for candoxin [70] and explained by the absence of an Asp residue at position 31 (homologous to position 30 in αδ-BgTxs; Fig. 2). However, all αδ-BgTx variants contain an Asp-residue at this position. Therefore, the reversibility of αδ-BgTx actions warrants further investigation.

The discovery of αδ-BgTxs underscores the relevance and potential of snake venoms as a source of novel nicotinic receptor probes ([22], reviewed in [9-10]), especially in view of the fact that the venoms of the majority of snake species are still unexplored. However, even in the well-studied venoms of species like *B. multicinctus* or *N. kaouthia*, the high molecular diversity of snake neurotoxins offers great opportunities to isolate novel polypeptides (e.g., [57,71-72]) for dissecting the structure-function relationships of acetylcholine receptors and to label particular receptor subtypes. In analogy to chemical modifications of known toxins or of recombinant chimeric toxins, systematic studies of natural toxin subfamilies comprising ligands of nicotinic

receptors that differ only in a few substitutions may lead to additional insights and provide valuable tools to distinguish binding sites and receptor subtypes of different species.

Acknowledgments

We thank Dr. Tamotsu Omori-Satoh (Queen Saovabha Memorial Institute, Bangkok, Thailand), Dr. Yuji Samejima (Hoshi University, Tokyo, Japan) and Dr. Yuan Ming Chen (Department of Pharmacology, College of Medicine, National Taiwan University, Taipei, Taiwan) for their help with experiments and fruitful discussions.

Competing Interests

The authors declare that there are no competing interests associated with the manuscript.

Funding

This work was supported by grants of the Swedish Research Council (project 03X-3532), the

research funding programme “LOEWE − Landes-Offensive zur Entwicklung Wissenschaftlich-ökonomischer Exzellenz" of the Ministry of Higher Education, Research and the Arts of the State of Hesse, Germany, and partially by the Russian Foundation for Basic Research (No. 17-00-00063, 18-04-01366 and 18-04-01075). The funders had no role in study design, data collection and analysis, decision to publish, or preparation of the manuscript.

Author contribution

YU, UK, DM, TB and VT designed the experiments. YU, UK, IK, DL, EC, BM, IP, II, NP and RZ performed the experiments. YU, UK, IK, HJ, GA, DM, TB and VT analyzed the data. LC and DAW provided key reagents; and YU, UK, DM and VT wrote the manuscript. All authors revised and approved the final manuscript.

References

1. Cecchini, M. and Changeux, J.P. (2015) The nicotinic acetylcholine receptor and its prokaryotic homologues: Structure, conformational transitions and allosteric modulation. *Neuropharmacology* **96,** 137-149 https://doi.org/10.1016/j.neuropharm.2014.12.006

2. Chen, L. (2010) In pursuit of the high-resolution structure of nicotinic acetylcholine receptors. *J. Physiol*. **588**, 557–564 https://doi.org/10.1113/jphysiol.2009.184085

3. Tsetlin, V. and Hucho, F. (2009) Nicotinic acetylcholine receptors at atomic resolution. *Curr. Opin. Pharmacol.* **9**, 306–310 https://doi.org/10.1016/j.coph.2009.03.005

4. Karlin, A. (2002) Emerging structure of the nicotinic acetylcholine receptors. *Nature Rev. Neurosci*. **3**, 102–114 https://doi.org/10.1038/nrn731

5. Unwin, N. (2003) Structure and action of the nicotinic acetylcholine receptor explored by electron microscopy. *FEBS Lett*. **555**, 91–95 PMID:14630325

6. Kalamida, D., Poulas, K., Avramopoulou, V., Fostieri, E., Lagoumintzis, G., Lazaridis, K., Sideri, A., Zouridakis, M. and Tzartos, S.J. (2007) Muscle and neuronal nicotinic acetylcholine receptors. Structure, function and pathogenicity. *FEBS J.* **274**, 3799–3845 https://doi.org/10.1111/j.1742-4658.2007.05935.x

7. Le Dain, A.C., Madsen, B.W. and Edeson, R.O. (1991) Kinetics of (+)-tubocurarine blockade at the neuromuscular junction. *Br. J. Pharmacol*. **103**, 1607-1613 PMID:1884116

8. Taly, A. and Charon, S. (2012) α7 nicotinic acetylcholine receptors: a therapeutic target in the structure era. *Curr. Drug Targets* **13**, 695–706 PMID:22300037

9. Endo, T. and Tamiya, N. Structure–function relationships of postsynaptic neurotoxins from snake venoms. In: Harvey AL, editor. Snake Toxins. New York: Pergamon Press; 1991. pp. 165–222.

10. Tsetlin, V.I. and Hucho, F. (2004) Snake and snail toxins acting on nicotinic acetylcholine receptors: fundamental aspects and medical applications. *FEBS Lett*. **557**, 9–13. PMID:14741333

11. Tsetlin, V.I. (2015) Three-finger snake neurotoxins and Ly6 proteins targeting nicotinic acetylcholine receptors: pharmacological tools and endogenous modulators. *Trends Pharmacol. Sci.* **36**, 109-23 https://doi.org/10.1016/j.tips.2014.11.003

12. Utkin, Y.N., Kukhtina, V.V., Kryukova, E.V., Chiodini, F., Bertrand, D., Methfessel, C. and Tsetlin, V.I. (2001) "Weak toxin" from *Naja kaouthia* is a nontoxic antagonist of alpha 7 and muscle-type nicotinic acetylcholine receptors. *J. Biol. Chem.* **276**, 15810–15815 https://doi.org/10.1074/jbc.M100788200

13. Pawlak, J., Mackessy, S.P., Fry, B.G., Bhatia, M., Mourier, G., Fruchart-Gaillard, C., Servent, D., Ménez, R., Stura, E., Ménez, A. and Kini, R.M. (2006) Denmotoxin, a three-finger toxin from the colubrid snake *Boiga dendrophila* (Mangrove Catsnake) with bird-specific activity. *J. Biol. Chem*. **281**, 29030–29041 https://doi.org/10.1074/jbc.M605850200

14. Chang, C.C. and Lee, C.Y. (1963) Isolation of neurotoxins from the venom of *Bungarus multicinctus* and their modes of neuromuscular blocking action. *Arch. Int. Pharmacodyn. Ther*. **144**, 241–257 PMID:4043649

15. Mebs, D., Narita, K., Iwanaga, S., Samejima, Y. and Lee C.Y. (1972) Purification, properties and amino acid sequence of α-bungarotoxin from the venom of *Bungarus multicinctus*. *Hoppe-Seyler's Z. Physiol. Chem.* **353**, 243–262 https://doi.org/10.1515/bchm2.1972.353.1.243

16. Changeux, J.P., Kasai, M. and Lee, C.Y. (1970) Use of a snake venom toxin to characterize the cholinergic receptor protein. *Proc. Natl. Acad. Sci. USA* **67**, 1241–1247. PMID:5274453

17. Sher, E., Giovannini, F., Boot, J. and Lang, B. (2000) Peptide neurotoxins, small-cell lung carcinoma and neurological paraneoplastic syndromes. *Biochimie* **82**, 927–936 https://doi.org/10.1016/S0300-9084(00)01165-2

18. Lebbe, E.K., Peigneur, S., Wijesekara, I. and Tytgat, J. (2014) Conotoxins targeting nicotinic acetylcholine receptors: an overview. *Mar. Drugs* **12**, 2970-3004 https://doi.org/10.3390/md12052970

19. Muttenthaler, M., Akondi, K.B., Alewood, P.F. (2011) Structure-activity studies on alpha-conotoxins. *Curr. Pharm. Des.* **17**, 4226–4241 https://doi.org/10.2174/138161211798999384

20. Kasheverov, I.E., Utkin, Y.N. and Tsetlin, V.I. (2009) Naturally occurring and synthetic peptides acting on nicotinic acetylcholine receptors. *Curr. Pharm. Des.* **15,** 2430–2452 http://dx.doi.org/10.2174/138161209788682316

21. Schmidt, J.J., Weinstein, S.A. and Smith L.A. (1992) Molecular properties and structure-function relationships of lethal peptides from venom of Wagler's pit viper, *Trimeresurus wagleri*.

22. Utkin, Y.N., Weise, C., Kasheverov, I.E., Andreeva, T.V., Kryukova, E.V., Zhmak, M.N., Starkov, V.G., Hoang, N.A., Bertrand, D., Ramerstorfer, J., Sieghart, W., Thompson, A.J., Lummis, S.C. and Tsetlin V.I. (2012) Azemiopsin from *Azemiops feae* viper venom, a novel polypeptide ligand of nicotinic acetylcholine receptor. *J. Biol. Chem*. **287**, 27079–27086 https://doi.org/10.1074/jbc.M112.363051

23. Groebe, D.R., Dumm, J.M., Levitan, E.S. and Abramson, S.N. (1995) alpha-Conotoxins selectively inhibit one of the two acetylcholine binding sites of nicotinic receptors. *Mol. Pharmacol*. **48**, 105–111 PMID: 7623764

24. McArdle, J.J., Lentz, T.L., Witzemann, V., Schwarz, H., Weinstein, S.A. and Schmidt, J.J. (1999) Waglerin-1 selectively blocks the epsilon form of the muscle nicotinic acetylcholine receptor. *J. Pharmacol. Exp. Ther*. **289**, 543–550 PMID:10087048

25. Molles, B.E., Rezai, P., Kline, E.F., McArdle, J.J., Sine, S.M. and Taylor P. (2002) Identification of residues at the alpha and epsilon subunit interfaces mediating species selectivity of Waglerin-1 for nicotinic acetylcholine receptors. *J. Biol. Chem*. **277**, 5433–5440 https://doi.org/10.1074/jbc.M109232200

26. Kuch, U., Molles, B.E., Satoh, T., Chanhome, L., Samejima, Y. and Mebs, D. (2003) Identification of alpha-bungarotoxin (A31) as the major postsynaptic neurotoxin, and complete nucleotide identity of a genomic DNA of *Bungarus candidus* from Java with exons of the

Bungarus multicinctus alpha-bungarotoxin (A31) gene. *Toxicon* **42**, 381–390 https://doi.org/10.1016/S0041-0101(03)00168-5

27. Chang, L.S., Lin, S.K., Huang, H.B. and Hsiao M. (1999) Genetic organization of α-bungarotoxins from *Bungarus multicinctus* (Taiwan banded krait): evidence showing that the production of α-bungarotoxin isotoxins is not derived from edited mRNAs. *Nucleic Acids Res.* **27**, 3970–3975 PMID:10497260

28. Chang, L.S., Lin, J., Chou, Y.C. and Hong E. (1997) Genomic structures of cardiotoxin 4 and cobrotoxin from *Naja naja atra* (Taiwan cobra). *Biochem. Biophys. Res. Commun* **239**, 756–762 https://doi.org/10.1006/bbrc.1997.7549

29. Altschul, S.F., Madden, T.F., Schaffer, A.A., Zhang, J., Zhang, Z., Miller, W. and Lipman, D.J. (1997) Gapped BLAST and PSI-BLAST: a new generation of protein database search programs. *Nucleic Acids Res*. **25**, 3389–3402 PMID:9254694

30. Swiss Institute of Bioinformatics ExPASy (Expert Protein Analysis System) Proteomics Server: Compute pI/Mw Tool. Available from: http://www.expasy.org/tools/pi_tool.html (accessed: 27 October 2018).

31. Reed, L.J. and Muench H. (1938) A simple method of estimating fifty percent endpoints. *Amer. J. Hyg*. **27**, 493–497 https://doi.org/10.1093/oxfordjournals.aje.a118408

32. Pizzi, M. (1950) Sampling variation of the fifty percent end-point, determined by the Reed-Muench (Behrens) method. *Hum. Biol*. **22**, 151–190 https://www.jstor.org/stable/41447976

33. Lee, C.Y., Chen, Y.M. and Mebs D. (1976) Chromatographic separation of the venom of *Bungarus caeruleus* and pharmacologic characterization of its components. *Toxicon* **14**, 451–457 https://doi.org/10.1016/0041-0101(76)90062-3

34. Kasheverov, I.E., Chugunov, A.O., Kudryavtsev, D.S., Ivanov, I.A., Zhmak, M.N., Shelukhina, I.V., Spirova, E.N., Tabakmakher,V.M., Zelepuga, E.A., Efremov, R.G. and Tsetlin,

V.I. (2016) High-affinity α-conotoxin PnIA analogs designed on the basis of the protein surface topography method. *Sci. Rep.***6**, 36848 doi: 10.1038/srep36848

35. Lee, B.S., Gunn, R.B. and Kopito, R.R. (1991) Functional differences among nonerythroid anion exchangers expressed in a transfected human cell line. *J. Biol. Chem*. **266**, 11448–11454. PMID: 2050661

36. Sine, S.M. (1993) Molecular dissection of subunit interfaces in the acetylcholine receptor: identification of residues that determine curare selectivity. *Proc. Natl. Acad. Sci. USA* **90**, 9436–9440 PMID:8415719

37. Sugiyama, N., Marchot, P., Kawanishi, C., Osaka, H., Molles, B., Sine, S.M. and Taylor P. (1998) Residues at the subunit interfaces of the nicotinic acetylcholine receptor that contribute to α-conotoxin M1 binding. *Mol. Pharmacol*. **53**, 787–794 https://doi.org/10.1124/mol.53.4.787

38. Ziganshin, R.H., Kovalchuk, S.I., Arapidi, G.P., Starkov, V.G., Hoang, A.N., Thi Nguyen, T.T., Nguyen, K.C., Shoibonov, B.B., Tsetlin, V.I. and Utkin, Y.N. (2015) Quantitative proteomic analysis of Vietnamese krait venoms: Neurotoxins are the major components in *Bungarus multicinctus* and phospholipases A2 in *Bungarus fasciatus*. *Toxicon* **107**, 197-209. https://doi.org/10.1016/j.toxicon.2015.08.026.

39. Ackermann, E.J. and Taylor P. (1997) Nonidentity of the alpha-neurotoxin binding sites on the nicotinic acetylcholine receptor revealed by modification in alpha-neurotoxin and receptor structures. *Biochemistry* **36**, 12836–12844 https://doi.org/10.1021/bi971513u

40. Shelukhina, I.V., Zhmak, M.N., Lobanov, A.V., Ivanov, I.A., Garifulina, A.I., Kravchenko, I.N., Rasskazova, E.A., Salmova, M.A., Tukhovskaya, E.A., Rykov, V.A., Slashcheva, G.A., Egorova, N.S., Muzyka, I.S., Tsetlin, V.I. and Utkin Y.N. (2018) Azemiopsin, a selective peptide antagonist of muscle nicotinic acetylcholine receptor: preclinical evaluation as a local muscle relaxant. *Toxins (Basel)* **10**, pii: E34 https://doi.org/10.3390/toxins10010034

41. Dellisanti, C.D., Yao, Y., Stroud, J.C., Wang, Z.Z. and Chen L. (2007) Crystal structure of the extracellular domain of nAChR alpha1 bound to alpha-bungarotoxin at 1.94 A resolution.

42. Marti-Renom, M.A., Stuart, A., Fiser, A., Sanchez, R., Melo, F. and Sali A. (2000) Comparative protein structure modeling of genes and genomes. *Annu. Rev. Biophys. Biomol. Struct.* **29**, 291–325 https://doi.org/10.1146/annurev.biophys.29.1.291

43. Bourne, Y., Talley, T.T., Hansen, S.B., Taylor, P. and Marchot P. (2005) Crystal structure of a Cbtx-AChBP complex reveals essential interactions between snake α-neurotoxins and nicotinic receptors. *EMBO J*. **24**, 1512–1522 https://doi.org/10.1038/sj.emboj.7600620

44. Unwin, N. (2005) Refined structure of the nicotinic acetylcholine receptor at 4A resolution.

45. Ritchie, D.W., Kozakov, D. and Vajda S. (2008) Accelerating and focusing protein–protein docking correlations using multi-dimensional rotational FFT generating functions. *Bioinformatics* **24**, 1865–1873 https://doi.org/10.1093/bioinformatics/btn334

46. Lachumanan, R., Armugam, A., Tan, C.H. and Jeyaseelan K. (1998) Structure and organization of the cardiotoxin genes in *Naja naja sputatrix*. *FEBS Lett* **433**, 119–124 https://doi.org/10.1016/S0014-5793(98)00894-1

47. Afifiyan, F., Armugam, A., Tan, C.H., Gopalakrishnakone, P. and Jeyaseelan K. (1999) Postsynaptic α-neurotoxin gene of the spitting cobra, *Naja naja sputatrix*: structure, organization, and phylogenetic analysis. *Genome Res*. **9**, 259–266 https://doi.org/10.1101/gr.9.3.259

48. Fujimi, T.J., Nakajyo, T., Nishimura, E., Ogura, E., Tsuchiya, T., Tamiya, T. (2003) Molecular evolution and diversification of snake toxin genes, revealed by analysis of intron sequences. *Gene* **313**:111-118.

49. Chang, C.C. The action of snake venom on nerve and muscle. In: Lee CY, editor. Snake Venoms. Berlin: Springer; 1979. pp. 309–376.

50. Cheng, Y. and Prusoff, W.H. (1973) Relationship between the inhibition constant (*KI*) and the concentration of inhibitor which causes 50 per cent inhibition (*IC*50) of an enzymatic reaction. *Biochem. Pharmacol*. **22**, 3099–3108 https://doi.org/10.1016/0006-2952(73)90196-2

51. Spirova, E.N., Ivanov, I.A., Kasheverov, I.E., Kudryavtsev, D.S., Shelukhina, I.V., Garifulina, A.I., Son, L.V., Lummis, S.C.R., Malca-Garcia, G.R., Bussmann, R.W., Hennig, L., Giannis, A., Tsetlin, V.I. (2019) Curare alkaloids from Matis Dart Poison: Comparison with d-tubocurarine in interactions with nicotinic, 5-HT3 serotonin and GABAA receptors. *PLoS One*. **14**, e0210182. http://doi.org/10.1371/journal.pone.0210182.

52. Lebbe, E.K., Peigneur, S., Maiti, M., Mille, B.G., Devi, P., Ravichandran, S., Lescrinier, E., Waelkens, E., D'Souza, L., Herdewijn, P., Tytgat, J. (2014) Discovery of a new subclass of α-conotoxins in the venom of *Conus australis*. *Toxicon*. **91**, 145-154. http://doi.org/10.1016/j.toxicon.2014.08.074.

53. Fiordalisi, J.J., Grant, G.A. (1993) Evidence for a fast-exchange conformational process in alpha-bungarotoxin. *Toxicon*. **31**, 767-775.

54. Rjeibi, I., Mabrouk, K., Mosrati, H., Berenguer, C., Mejdoub, H., Villard, C., Laffitte, D., Bertin, D., Ouafik, L., Luis, J., Elayeb, M., Srairi-Abid, N. (2011) Purification, synthesis and characterization of AaCtx, the first chlorotoxin-like peptide from *Androctonus australis* scorpion venom. *Peptides.* **32**, 656-663. http://doi.org/10.1016/j.peptides.2011.01.015.

55. Fernández, J., Gutiérrez, J.M., Angulo, Y., Sanz, L., Juárez, P., Calvete, J.J., Lomonte, B. (2010) Isolation of an acidic phospholipase A2 from the venom of the snake *Bothrops asper* of Costa Rica: biochemical and toxicological characterization. *Biochimie.* **92**, 273-283. http://doi.org/10.1016/j.biochi.2009.12.006.

56. Romi, R., Crest, M., Gola, M., Sampieri, F., Jacquet, G., Zerrouk, H., Mansuelle, P., Sorokine, O., Van Dorsselaer, A., Rochat, H., Martin-Eauclaire, M.-F., Van Rietschoten, J.

(1993) Synthesis and characterization of kaliotoxin. Is the 26-32 sequence essential for potassium channel recognition? *J. Biol. Chem*. **268**, 26302-26309.

57. Wang, C.I., Reeks, T., Vetter, I., Vergara, I., Kovtun, O., Lewis, R.J., Alewood, P.F. and Durek, T. (2014) Isolation and structural and pharmacological characterization of α-elapitoxin-Dpp2d, an amidated three finger toxin from black mamba venom. *Biochemistry* **53**, 3758-3766 https://doi.org/10.1021/bi5004475

58. Bechis, G., Granier, C., Van Rietschoten, J., Jover, E., Rochat, H., Miranda, F. (1976) Purification of six neurotoxins from the venom of *Dendroaspis viridis*. Primary structure of two long toxins. *Eur. J. Biochem*. **68**, 445-456.

59. Zeng, H., Moise, L., Grant, M.A. and Hawrot, E. (2001) The solution structure of the complex formed between alpha-bungarotoxin and an 18-mer cognate peptide derived from the alpha 1 subunit of the nicotinic acetylcholine receptor from *Torpedo californica*. *J. Biol. Chem*. **276**, 22930-22940 https://doi.org/10.1074/jbc.M102300200

60. Samson, A., Scherf, T., Eisenstein, M., Chill, J. and Anglister, J. (2002) The mechanism for acetylcholine receptor inhibition by alpha-neurotoxins and species-specific resistance to alpha-bungarotoxin revealed by NMR. *Neuron* **35**, 319–332 https://doi.org/10.1016/S0896-6273(02)00773-0

61. Moise, L., Piserchio, A., Basus, V.J. and Hawrot E. (2002) NMR structural analysis of alpha-bungarotoxin and its complex with the principal alpha-neurotoxin-binding sequence on the alpha 7 subunit of a neuronal nicotinic acetylcholine receptor. *J. Biol. Chem*. **277**, 12406–12417 https://doi.org/10.1074/jbc.M110320200

62. Scherf, T., Balass, M., Fuchs, S., Katchalski-Katzir, E. and Anglister, J. (1997) Three-dimensional solution structure of the complex of alpha-bungarotoxin with a library-derived peptide. *Proc. Natl. Acad. Sci. USA* **94**, 6059–6064 https://doi.org/10.1073/pnas.94.12.6059

63. Scarselli, M., Spiga, O., Ciutti, A., Bernini, A., Bracci, L., Lelli, B, Lozzi, L., Calamandrei, D., Di Maro, D., Klein, S. and Niccolai N. (2002) NMR structure of alpha-bungarotoxin free and bound to a mimotope of the nicotinic acetylcholine receptor. *Biochemistry* **41**, 1457-1463. https://doi.org/10.1021/bi011012f

64. Bernini, A., Ciutti, A., Spiga, O., Scarselli, M., Klein, S., Vannetti, S., Bracci, L., Lozzi, L., Lelli, B., Falciani, C., Neri, P. and Niccolai N. (2004) NMR and MD studies on the interaction between ligand peptides and alpha-bungarotoxin. *J. Mol. Biol*. **339**, 1169-1177 https://doi.org/10.1016/j.jmb.2004.04.041

65. Zouridakis, M., Giastas, P., Zarkadas, E., Chroni-Tzartou, D., Bregestovski, P. and Tzartos, S.J. (2014) Crystal structures of free and antagonist-bound states of human α9 nicotinic receptor extracellular domain. *Nat. Struct. Mol. Biol*. **21**, 976-980 https://doi.org/10.1038/nsmb.2900

66. Huang, S., Li, S.X., Bren, N., Cheng, K., Gomoto, R., Chen, L. and Sine, S.M. (2013) Complex between α-bungarotoxin and an α7 nicotinic receptor ligand-binding domain chimaera. *Biochem. J* **454**, 303-310 https://doi.org/10.1042/BJ20130636

67. Servent, D. and Menez, A. Snake neurotoxins that interact with nicotinic acetylcholine receptors. In: Massaro, E.J., editor. Handbook of Neurotoxicology, Vol. 1. Totowa, NJ: Humana Press; 2001. pp. 385–425.

68. Sine, S.M., Huang, S., Li, S.X., da Costa, C.J. and Chen, L. (2013) Inter-residue coupling contributes to high-affinity subtype-selective binding of α-bungarotoxin to nicotinic receptors.

69. Darveniza, P., Morgan-Hughes, J.A. and Thompson, E.J. (1979) Interaction of di-iodinated 125I-labelled alpha-bungarotoxin and reversible cholinergic ligands with intact synaptic acetylcholine receptors on isolated skeletal-muscle fibres from the rat. *Biochem. J*. **181**, 545-557 https://doi.org/10.1042/bj1810545

70. Nirthanan, S., Charpantier, E., Gopalakrishnakone, P., Gwee, M.C., Khoo, H.E., Cheah, L.S., Kini, R.M. and Bertrand, D. (2003) Neuromuscular effects of candoxin, a novel toxin from the venom of the Malayan krait (*Bungarus candidus*). *Br. J. Pharmacol*. 139, 832-844 https://doi.org/10.1042/bj1810545

71. Chung, C.L., Wu, B.N., Yang, C.C. and Chang L.S. (2002) Muscarinic toxin-like proteins from Taiwan banded krait (*Bungarus multicinctus*) venom: purification, characterization and gene organization. *Biol. Chem.* **383**, 1397–1406 https://doi.org/10.1515/BC.2002.158

72. Osipov, A.V., Kasheverov, I.E., Makarova, Y.V., Starkov, V.G., Vorontsova, O.V., Ziganshin, R.K., Andreeva, T.V., Serebryakova, M.V., Benoit, A., Hogg, R.C., Bertrand, D., Tsetlin, V.I. and Utkin, Y.N. (2008) Naturally occurring disulfide-bound dimers of three-fingered toxins: a paradigm for biological activity diversification. *J. Biol. Chem.* **283**, 14571–14580 https://doi.org/10.1074/jbc.M802085200

Table 1. Comparison of theoretical digestion fragments of toxin αδ-BgTx-2 deduced from the DNA sequence with those found in tryptic digest of isolated toxin.

Molecular masses (Da)			Sequence	Position in amino acid sequence of αδ-BgTx-2
Determined for		Calculated		
toxin of fraction 3	toxin of fraction 4			
2275.2	2275.2	2275.1	TPIPINAETCPPGENLCYTK	6-26
1616.8	1616.8	1617.0	KPYEEVTCCSTDK	52-64
1400.7	1400.7	1400.6	MWCDIWCSSR	27-36
1391.7	1391.8	1391.7	VVELGCAATCPS K	39-51
752.4	752.4	752.4	CNPHPK	65-70
696.4	696.4	696.4	LLCYK	1-5

Table 2. Comparison of neuromuscular blocking actions of αδ-BgTx-1 and α-BgTx from *Bungarus candidus* venom on the chick biventer cervicis nerve-muscle preparation.

Toxin	Concentration (nM)	Time (min) to neuromuscular block (mean±S.D. (number of experiments))	Acetylcholine response after neuromuscular block	Reversibility
αδ-BgTx-1	1250	11 ± 1 (3)	-	+
	125	38 ± 8 (4)	-	+
	37.6	86 ± 8 (4)	-	+
	12.5	> 300 (1)	-	+
α-BgTx	125	32 ± 5 (3)	-	-
	37.6	75 ± 3 (3)	-	-
	12.5	128 ± 17 (3)	-	-
	3.76	> 300 (2)	-	-

TABLE 3. K_i and nH values for binding of toxins to the *T. californica* and hα7 nAChRs.

Receptor	K_i, nM (nH)				
	α-BgTx	αδ-BgTx-1		αδ-BgTx-2	
		one site	two sites	one site	two sites
Torpedo	0.270 ± 0.013 (3.4 ± 0.5)	2.5 ± 0.4 (0.65 ± 0.07)	0.44 ± 0.22 7.5 ± 2.6	29 ± 3 (0.80 ± 0.09)	5.7 ± 1.9 80 ± 19
hα7	0.240 ± 0.031 (1.13 ± 0.13)	0.330 ± 0.014 (1.7 ± 0.1)	-	1.40 ± 0.16 (1.20 ± 0.14)	-

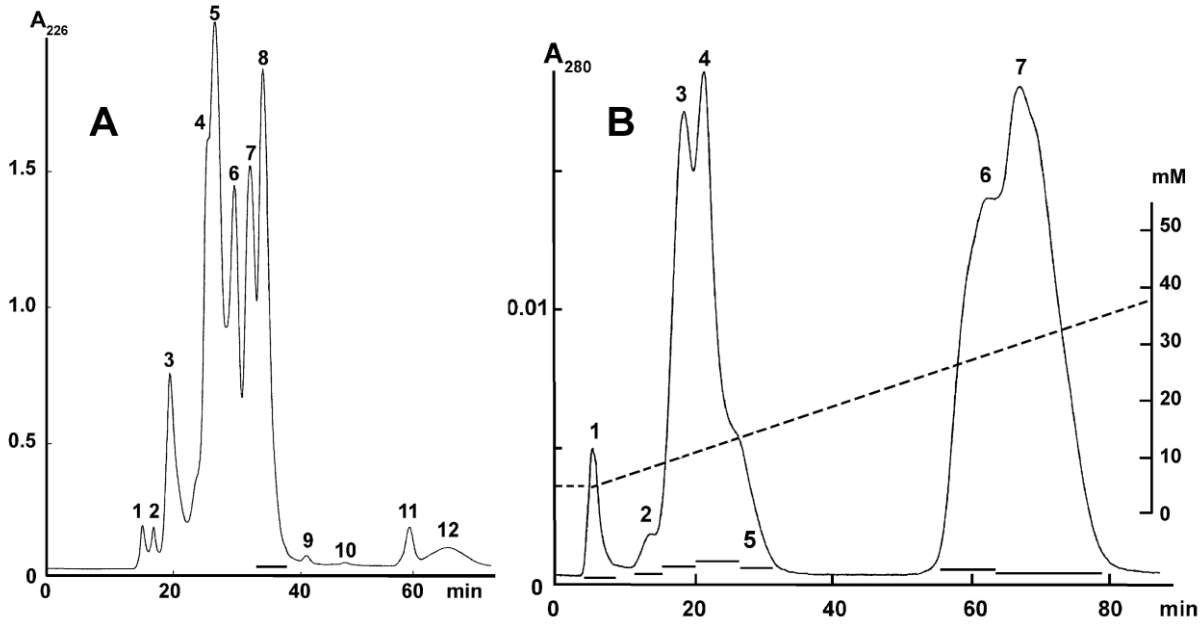

Figure 1. Liquid chromatography of crude *Bungarus candidus* venom from Thailand.

(A) Gel-filtration of crude venom on a Superdex 75 column (1 × 30 cm) eluted with 0.1 M ammonium acetate (pH 6.2) at a flow rate of 0.5 ml/min. Twelve major fractions were collected. (B) Cation-exchange chromatography of fraction 8 on a HEMA BIO 1000 CM column (8 × 250 mm, Tessek, Czech Republic) using a gradient of ammonium acetate concentration from 5 mM to 45 mM in 100 min at a flow rate of 1.0 ml/min. Dashed line indicates the concentration gradient generated at the input of the column.

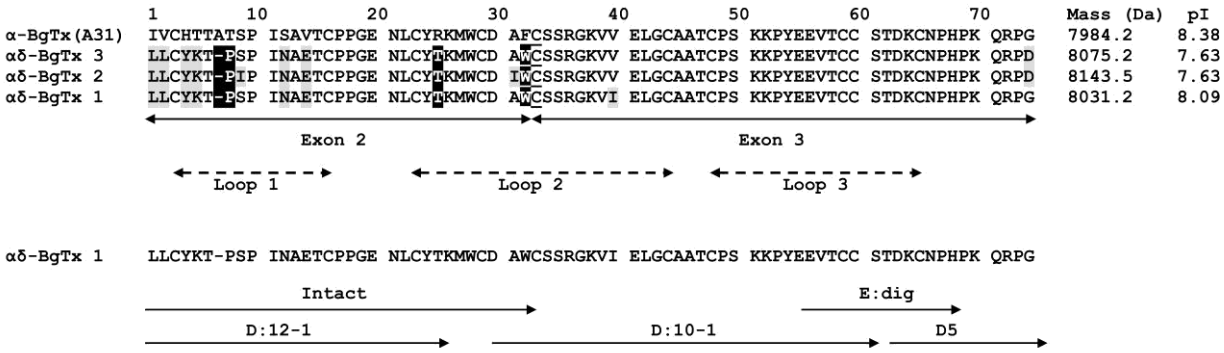

Figure 2. Amino acid sequence determination of αδ-BgTxs.

Top: Sequence alignment of *B. candidus* neurotoxins deduced from genomic DNA, their theoretical masses (corrected for the presence of five disulfide bonds) and isoelectric points. αδ-BgTx residues that differ from α-BgTx A31 are shaded; sequence differences that may be responsible for the different binding properties of αδ-BgTx-1 are shaded black; residues interrupted by introns are underlined. Bottom: Amino acid sequence of αδ-BgTx-1 obtained by Edman degradation. N-terminal sequencing of the native toxin was performed twice; further sequence analysis was performed using carboxymethylated αδ-BgTx-1 after digestion by Asp-N (indicated by D) and Glu-C (indicated by E) specific proteases and isolation of fragments by RP-HPLC (numbers refer to specific fractions).

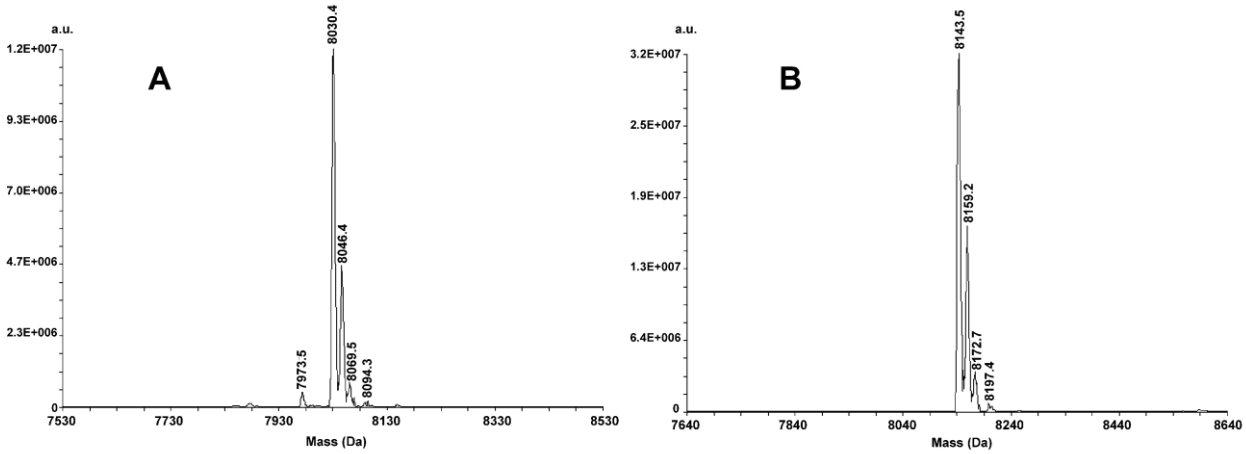

Figure 3. ESI-MS analyses of *B. candidus* αδ-BgTxs.

A - αδ-BgTx-1; B - αδ-BgTx-2.

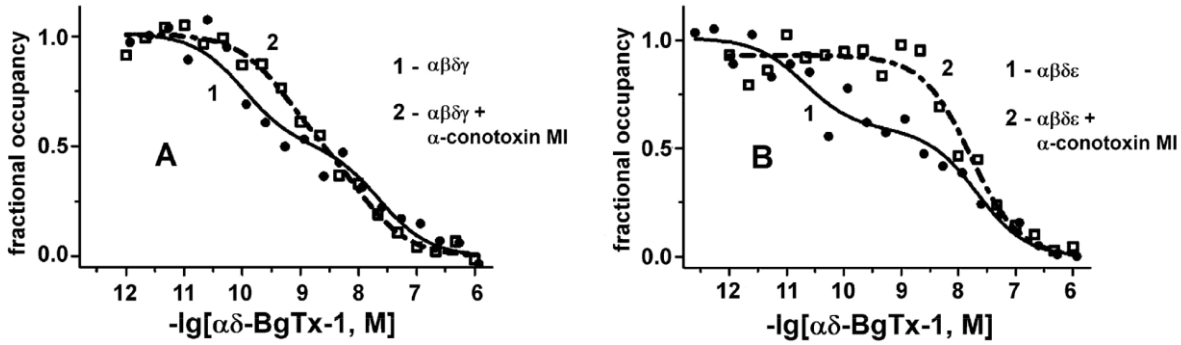

Figure 4. Competition binding curves for αδ-BgTx-1 with [^{125}I]α-BgTx initial binding rate to mouse muscle nAChRs transiently expressed in HEK293 cells, in the absence and presence of 30 nM α-conotoxin MI.

(A) Binding of αδ-BgTx-1 to embryonic form (α1β1δγ) nAChR. (B) Binding of αδ-BgTx-1 to adult form (α1β1δε) nAChR. Binding curves in the presence α-conotoxin MI display a right-ward shift only in the high-affinity site, indicating that the α−δ site is the high affinity site for αδ-BgTx-1.

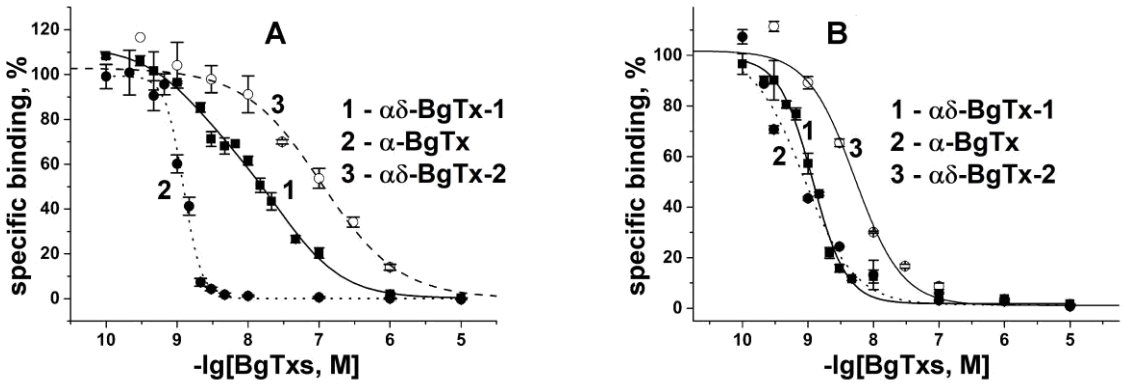

Figure 5. Competition of αδ-BgTxs and α-BgTx with [^{125}I]α-BgTx.

(A) Competition of αδ-BgTxs and α-BgTx with [^{125}I]α-BgTx for binding to *Torpedo californica* muscle-type nAChRs. (B) Competition of αδ-BgTxs and α-BgTx with [^{125}I]α-BgTx for binding neuronal hα7 nAChRs. 1 - αδ-BgTx-1, 2 - α-BgTx, 3 - αδ-BgTx-2.

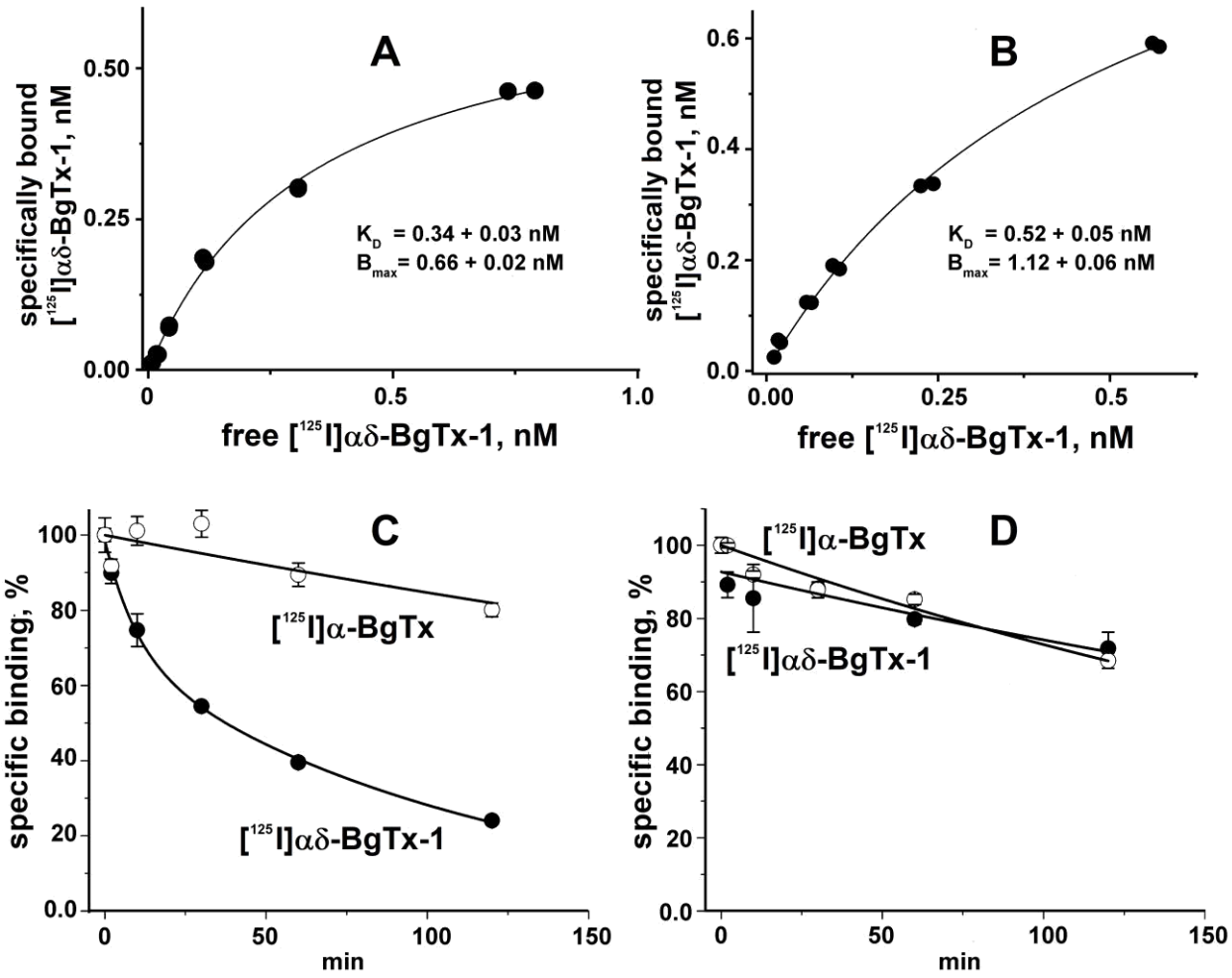

Figure 6. Direct radioligand assay of [^{125}I]αδ-BgTx-1 on *T. californica* muscle-type and neuronal hα7 nAChRs.

Saturation binding curves for [^{125}I]αδ-BgTx-1 (from 0.02 to 1.25 nM) interaction with the (A) *T. californica* α1β1δγ nAChR and (B) neuronal hα7 nAChR transfected in GH4C1 cells. The respective K_d and B_{max} values are shown calculated from a single experiment (duplicated for each point). Dissociation of BgTxs from complexes with *Torpedo* nAChR (C) and hα7 nAChR (D).

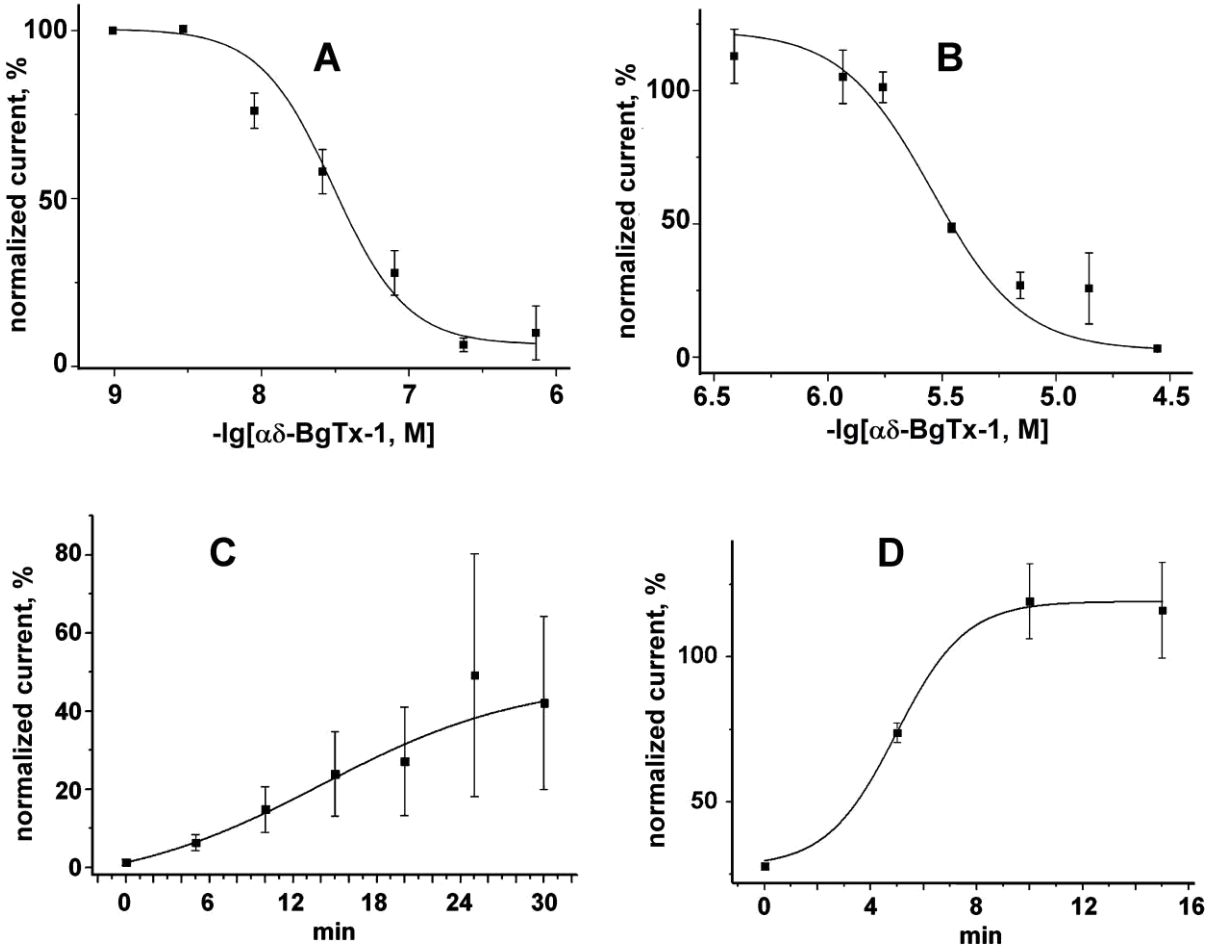

Figure 7. Electrophysiological assays on nAChRs heterologously expressed in *Xenopus* oocytes. Dose-response curve of αδ-BgTx-1 inhibitory action on the ACh-evoked (30 μM ACh) ionic current mediated by mouse muscle (A) or human neuronal α3β2 (B) nAChR. Oocytes were incubated with αδ-BgTx-1 for 10 min, followed by the application of 30 μM acetylcholine. All currents were normalized for the current evoked by 30 μM ACh. The IC50 values were 30 ± 9.8 nM (n = 5) and 2.9 ± 0.48 μM (n = 4) for muscle and α3β2 nAChR, respectively. Time course of the recovery of nAChR response to acetylcholine after the block produced by αδ-BgTx-1 in mouse muscle type (C) or neuronal α3β2 (D) nAChRs. Oocytes were incubated with 15.2 μM αδ-BgTx-1 for 10 min and then washed out at a flow rate of 0.4 ml/min. The response to 30 μM

acetylcholine before incubation with αδ-BgTx-1 was taken as 100% and was then registered every 5 min (n=3). Membrane potential was clamped at −60 mV.

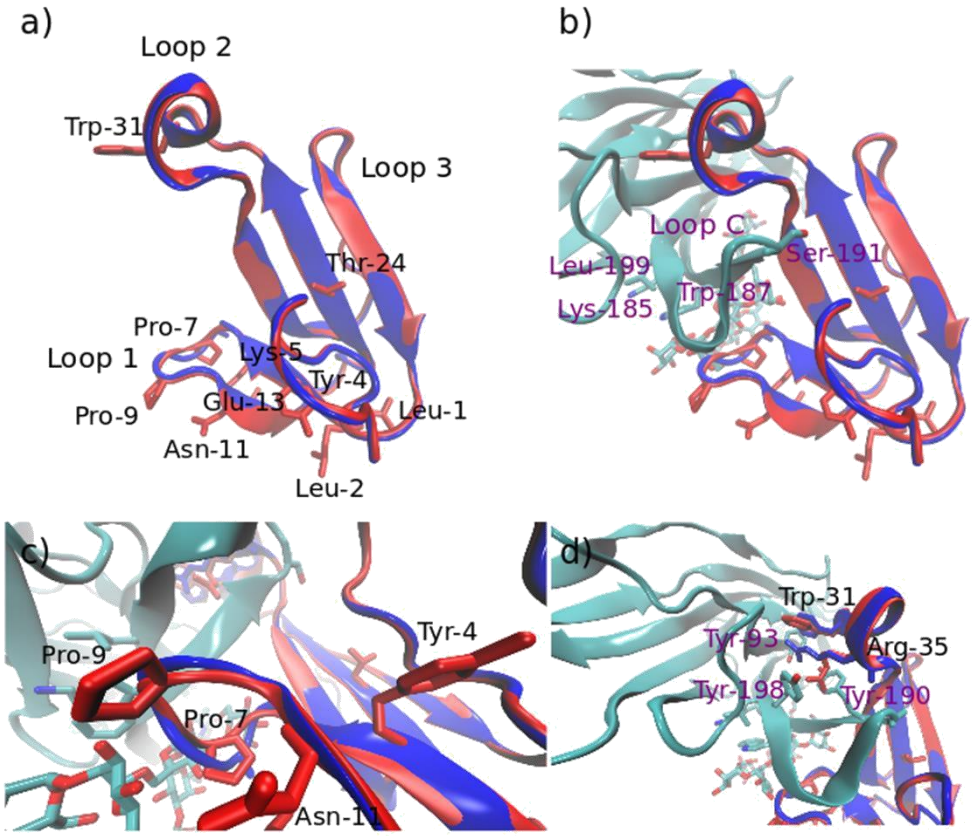

Figure 8. Comparison of the three-dimensional homology model of αδ-BgTx-1 (red) aligned with the α-BgTx (blue) template taken from the crystal structure of its complex with the extracellular domain of the nAChR subunit α1 [41].

Shown are (a) the free toxins aligned, (b) αδ-BgTx-1 aligned to α-BgTx as appearing in the X-ray structure in complex with the ligand-binding domain of nAChR subunit α1, (c) the loop 1 of both toxins in complex with the receptor enlarged, and (d) loop 2 of both toxins in that complex. Some of the important amino acid residues of αδ-BgTx-1 (black numbers) and the receptor (purple numbers) are highlighted. Note the slight difference in the spatial structure of the first loop with αδ-BgTx-1 exhibiting a sharper β-turn due to the deletion of A7 and the P8T substitution and the orientation of W31 and R35 (enumeration according to αδ-BgTx-1) in the hydrophobic box of the receptor residues.

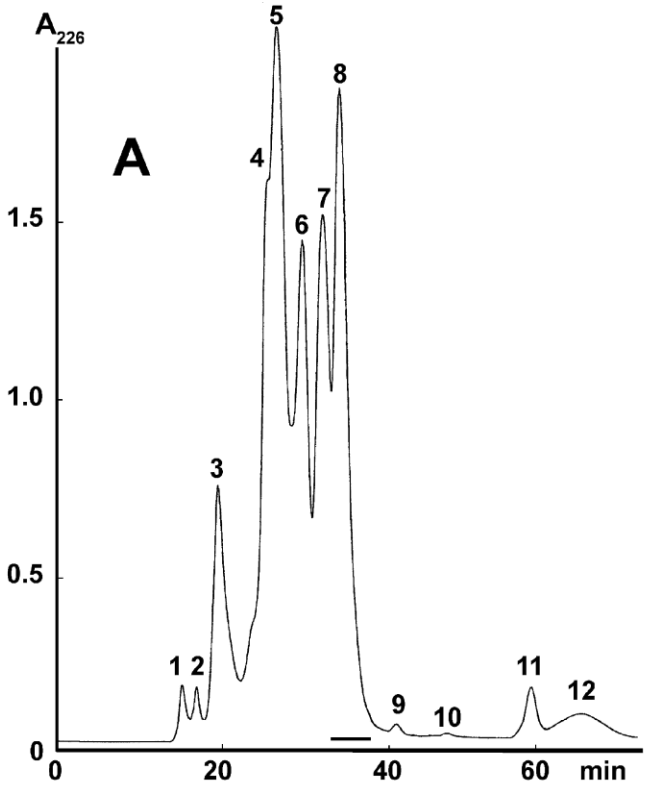
A
A_{226}
1.5
1.0
0.5
0
0
20
40
60
min
1
2
3
4
5
6
7
8
9
10
11
12

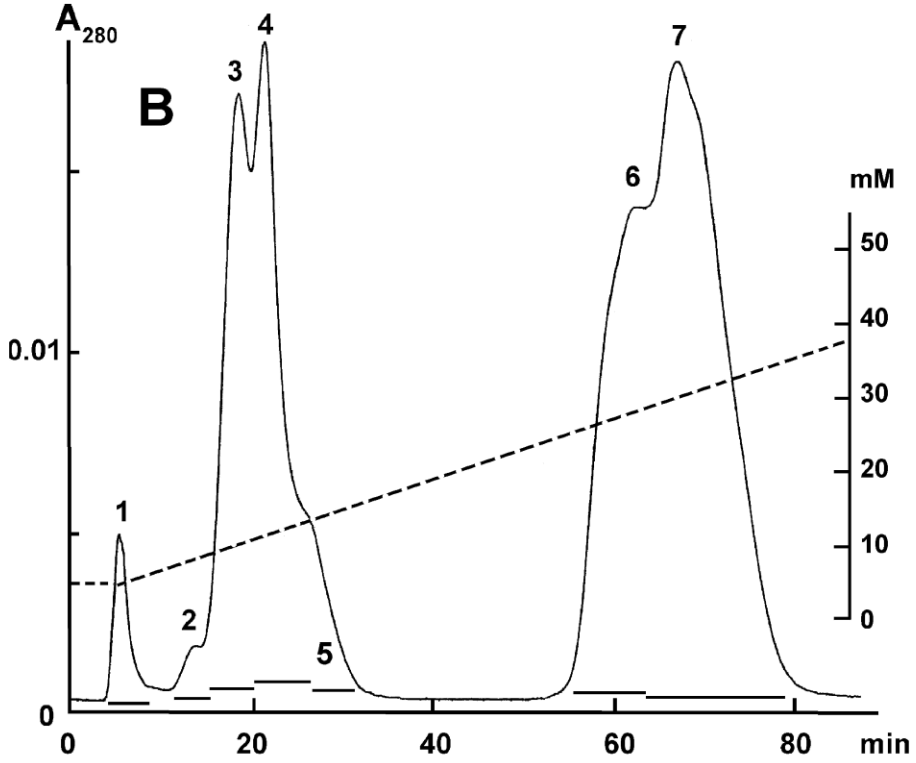
B
A_{280}
0.01
0
0
20
40
60
80
min
mM
50
40
30
20
10
0
1
2
3
4
5
6
7

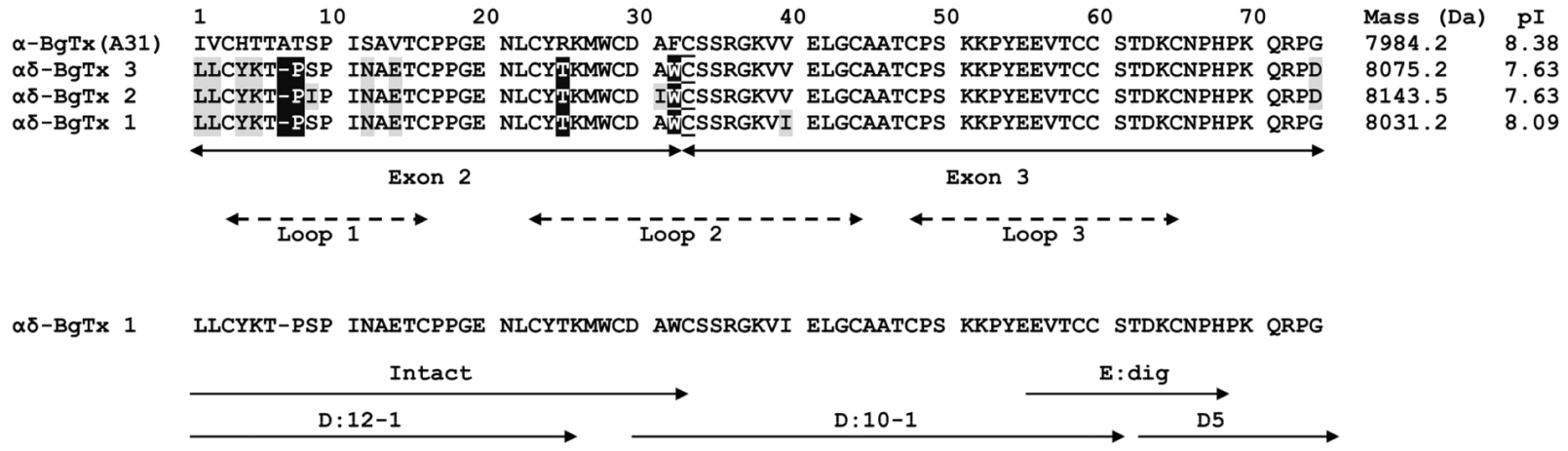
1 10 20 30 40 50 60 70 Mass (Da) pI
α-BgTx(A31) IVCHTTATSP ISAVTCPPGE NLCYRKMWCD AFCSSRGKVV ELGCAATCPS KKPYEEVTCC STDKCNPHPK QRPG 7984.2 8.38
αδ-BgTx 3 LLCYKT-PSP INAETCPPGE NLCYTKMWCD AWCSSRGKVV ELGCAATCPS KKPYEEVTCC STDKCNPHPK QRPD 8075.2 7.63
αδ-BgTx 2 LLCYKT-PIP INAETCPPGE NLCYTKMWCD IWCSSRGKVV ELGCAATCPS KKPYEEVTCC STDKCNPHPK QRPD 8143.5 7.63
αδ-BgTx 1 LLCYKT-PSP INAETCPPGE NLCYTKMWCD AWCSSRGKVI ELGCAATCPS KKPYEEVTCC STDKCNPHPK QRPG 8031.2 8.09
Exon 2
Exon 3
Loop 1
Loop 2
Loop 3

αδ-BgTx 1 LLCYKT-PSP INAETCPPGE NLCYTKMWCD AWCSSRGKVI ELGCAATCPS KKPYEEVTCC STDKCNPHPK QRPG
Intact
E:dig
D:12-1
D:10-1
D5

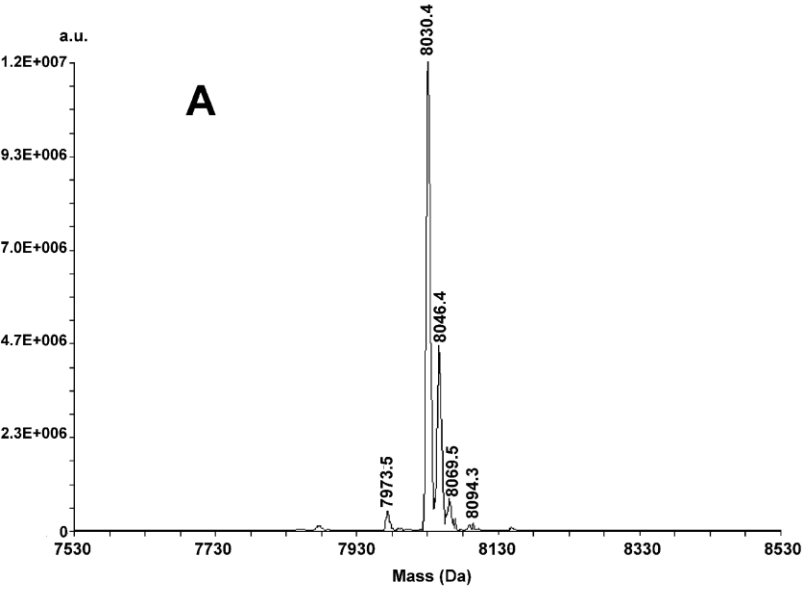
A
a.u.
1.2E+007
9.3E+006
7.0E+006
4.7E+006
2.3E+006
0
8030.4
8046.4
7973.5
8069.5
8094.3
7530
7730
7930
8130
8330
8530
Mass (Da)

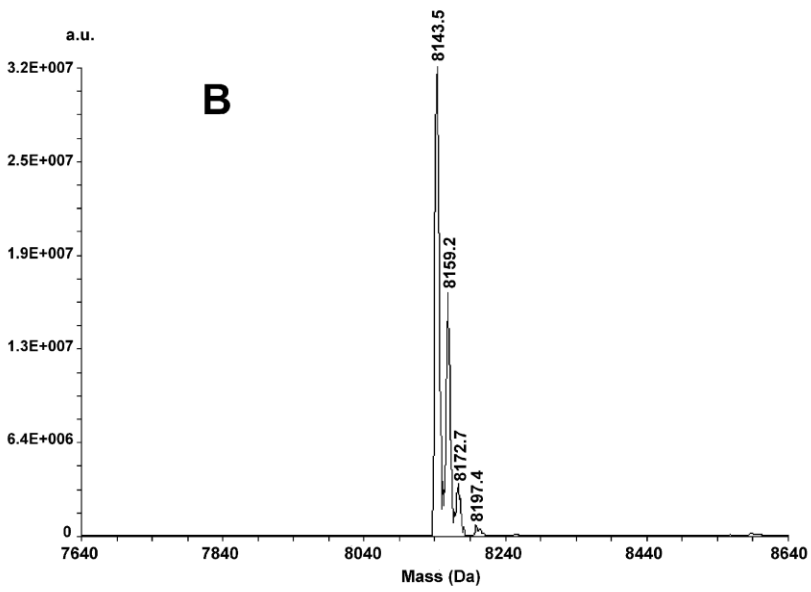
B
a.u.
3.2E+007
2.5E+007
1.9E+007
1.3E+007
6.4E+006
0
8143.5
8159.2
8172.7
8197.4
7640
7840
8040
8240
8440
8640
Mass (Da)

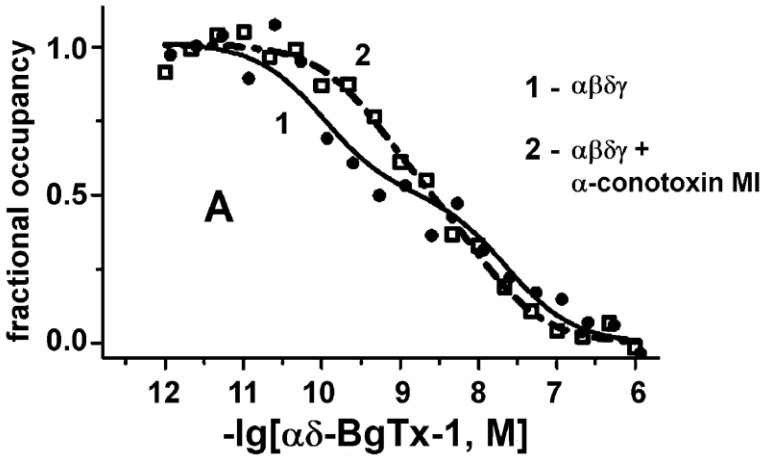
fractional occupancy
1.0
0.5
0.0
12
11
10
9
8
7
6
-lg[αδ-BgTx-1, M]
A
1
2
1 - αβδγ
2 - αβδγ +
α-conotoxin MI

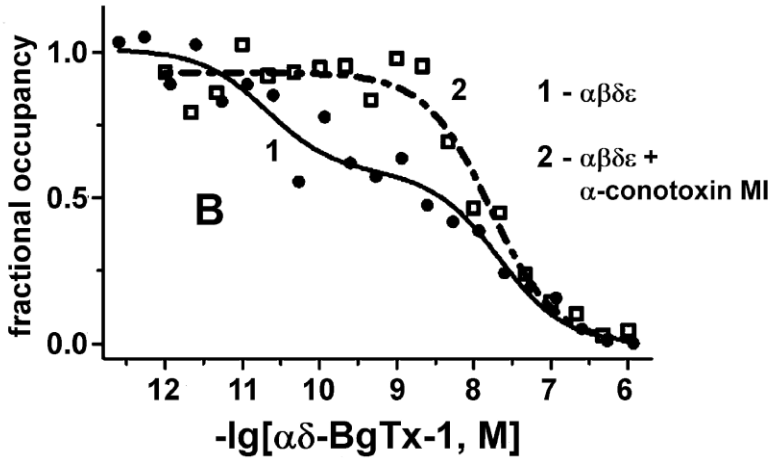
fractional occupancy
1.0
0.5
0.0
12
11
10
9
8
7
6
-lg[αδ-BgTx-1, M]
B
1
2
1 - αβδε
2 - αβδε +
α-conotoxin MI

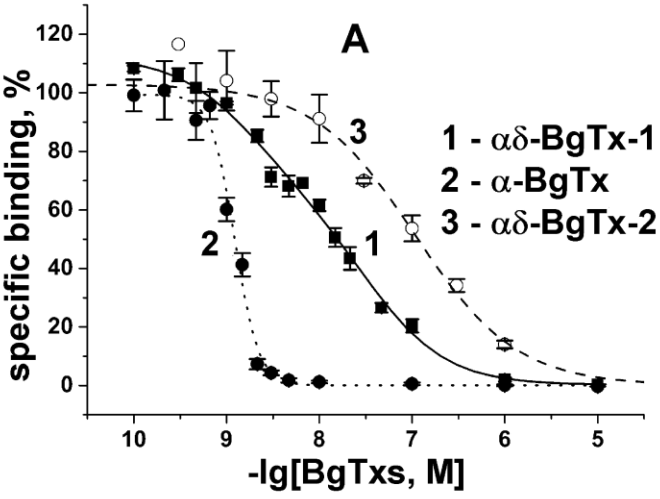
A
specific binding, %
-lg[BgTxs, M]
1 - αδ-BgTx-1
2 - α-BgTx
3 - αδ-BgTx-2
1
2
3

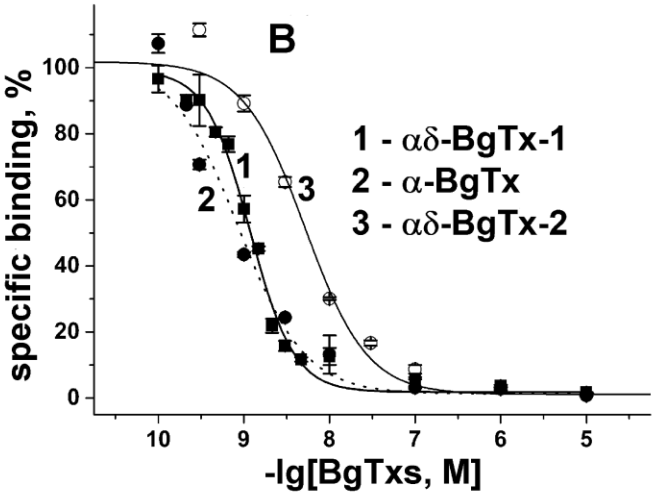
B
specific binding, %
-lg[BgTxs, M]
1 - αδ-BgTx-1
2 - α-BgTx
3 - αδ-BgTx-2
1
2
3

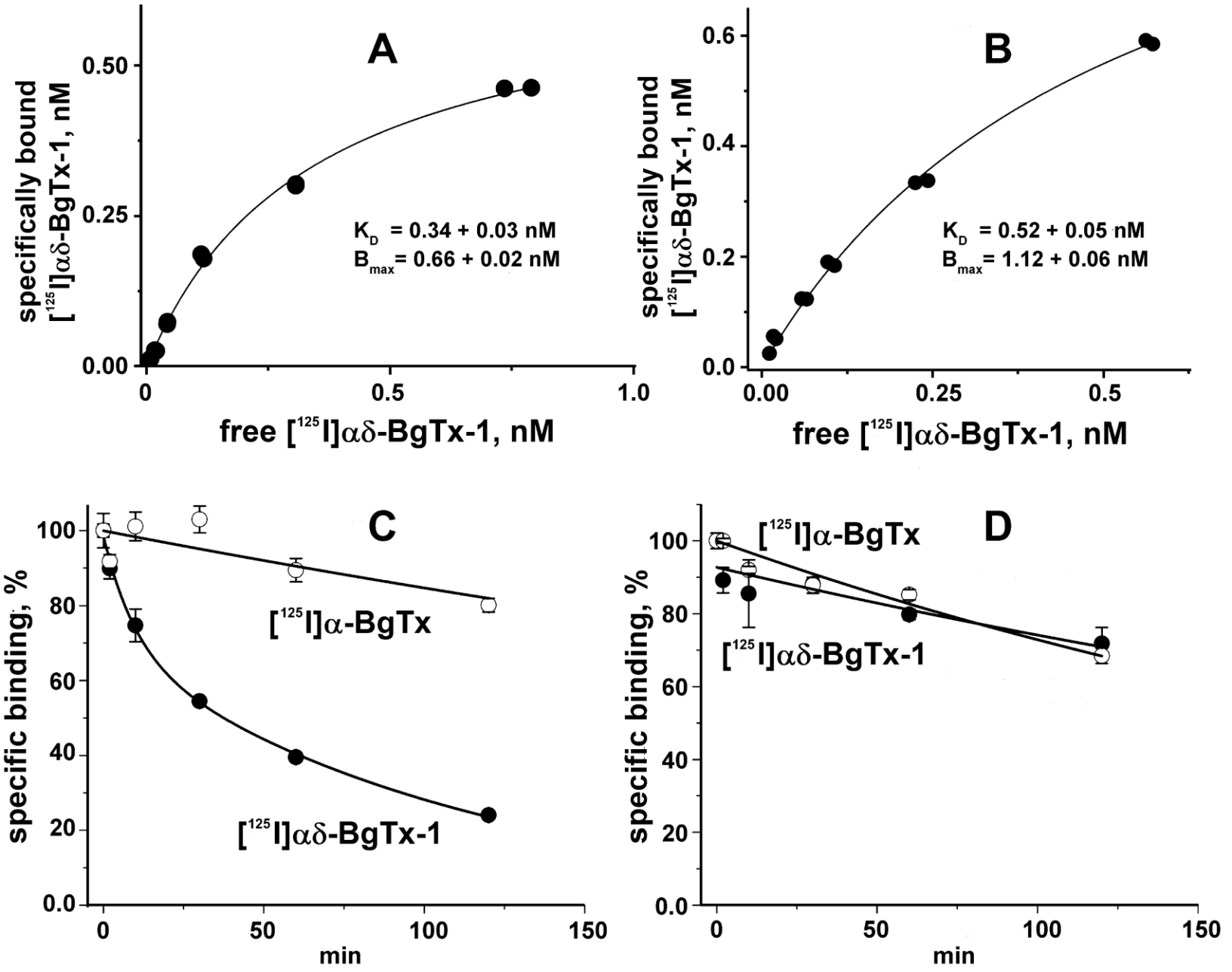
A
specifically bound [125I]αδ-BgTx-1, nM
0.50
0.25
0.00
0
0.5
1.0
free [125I]αδ-BgTx-1, nM
KD = 0.34 + 0.03 nM
Bmax = 0.66 + 0.02 nM
B
specifically bound [125I]αδ-BgTx-1, nM
0.6
0.4
0.2
0.0
0.00
0.25
0.5
free [125I]αδ-BgTx-1, nM
KD = 0.52 + 0.05 nM
Bmax = 1.12 + 0.06 nM
C
specific binding, %
100
80
60
40
20
0.0
0
50
100
150
min
[125I]α-BgTx
[125I]αδ-BgTx-1
D
specific binding, %
100
80
60
40
20
0.0
0
50
100
150
min
[125I]α-BgTx
[125I]αδ-BgTx-1

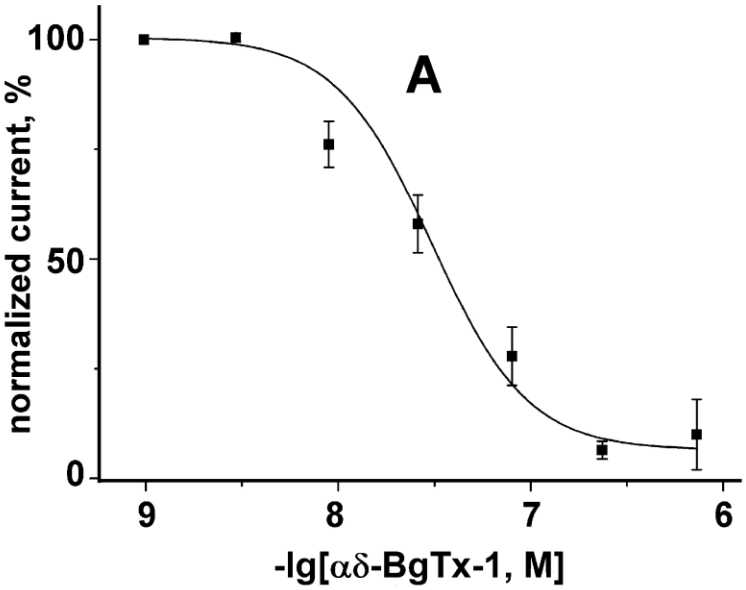
A
normalized current, %
100
50
0
9
8
7
6
-lg[αδ-BgTx-1, M]

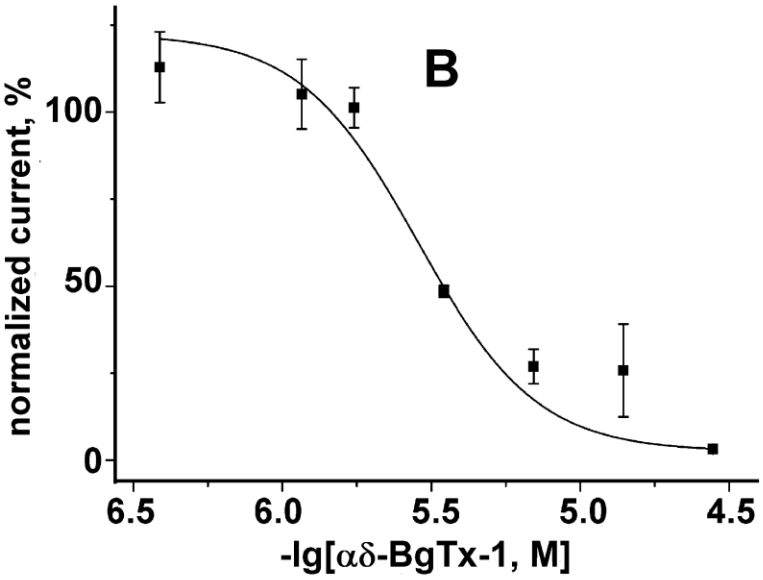
B
normalized current, %
100
50
0
6.5
6.0
5.5
5.0
4.5
-lg[αδ-BgTx-1, M]

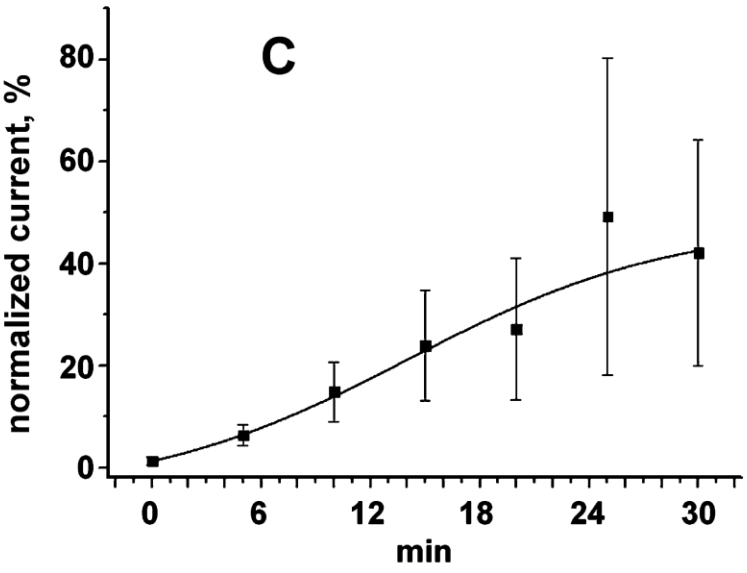
C
normalized current, %
80
60
40
20
0
0
6
12
18
24
30
min

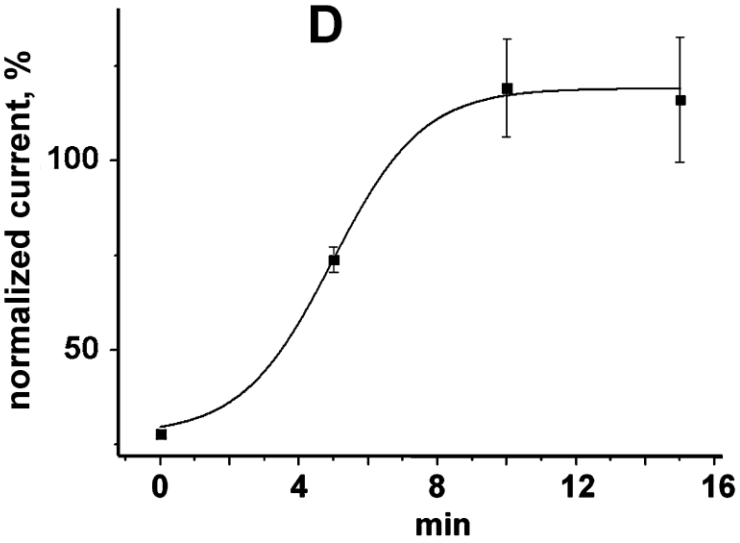
D
normalized current, %
100
50
0
4
8
12
16
min

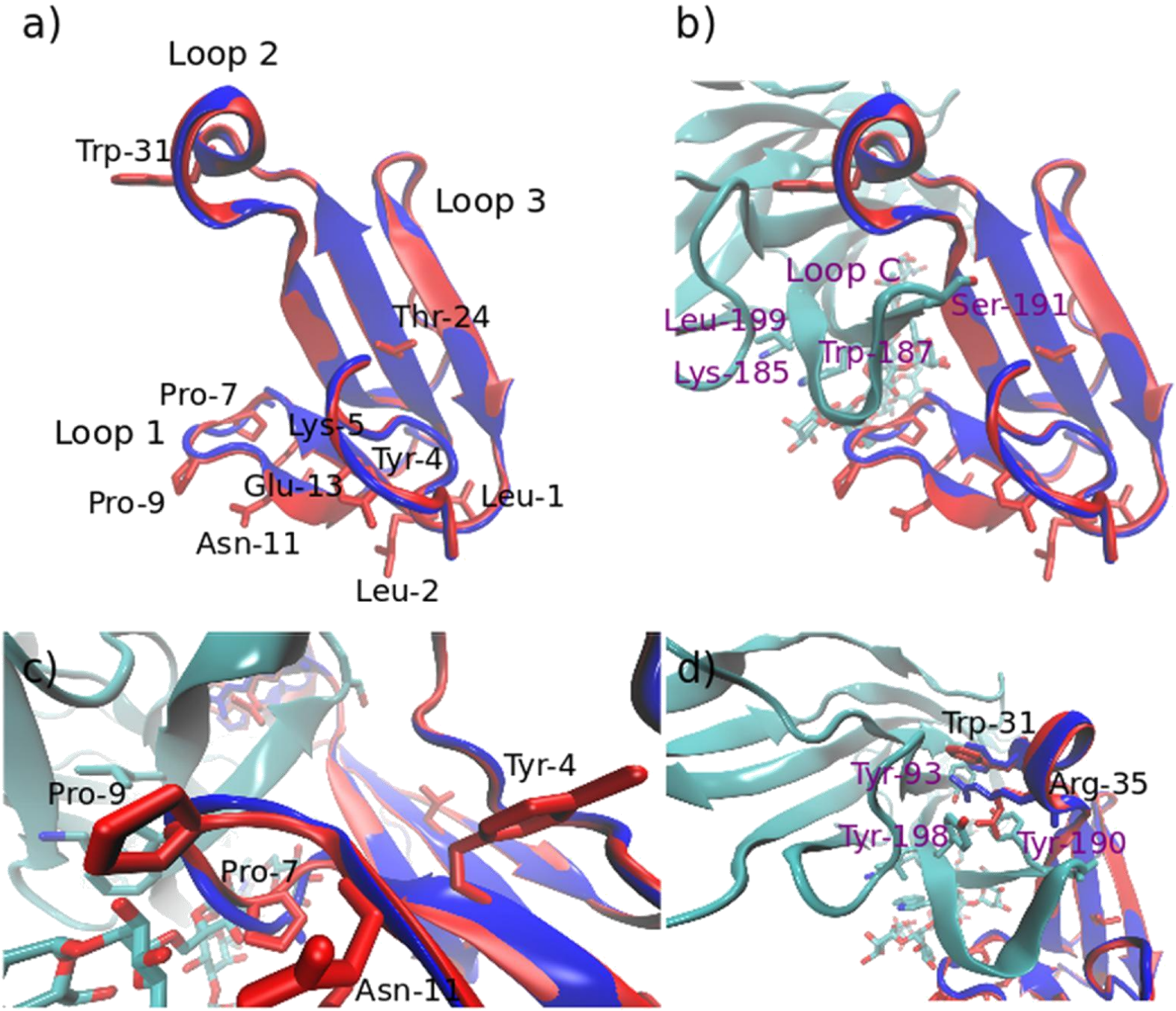
a)
Loop 2
Trp-31
Loop 3
Thr-24
Pro-7
Loop 1
Lys-5
Tyr-4
Glu-13
Pro-9
Leu-1
Asn-11
Leu-2
b)
Loop C
Leu-199
Ser-191
Trp-187
Lys-185
c)
Tyr-4
Pro-9
Pro-7
Asn-11
d)
Trp-31
Tyr-93
Arg-35
Tyr-198
Tyr-190

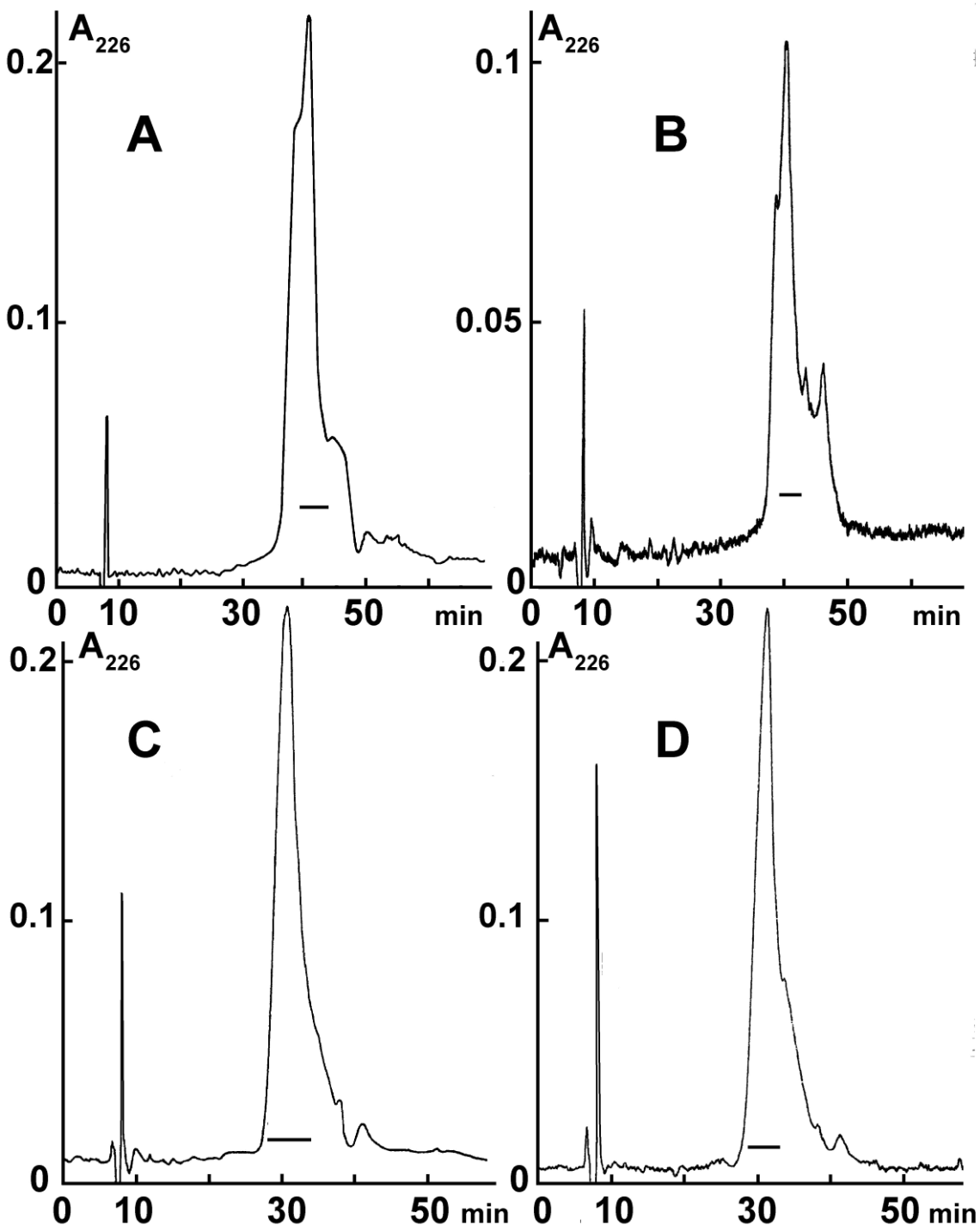

Supplementary Figure 1: Final purification of αδ-BgTx-1 (C and D) and αδ-BgTx-2 (A and B) by reversed phase HPLC.

Fractions obtained after ion-exchange chromatography (3, 4, 6 and 7 in Fig. 1B) were separated on a Phenomenex C_{18} column (10 250 mm) applying a gradient of 20% to 40 % (v/v, in 60 min) acetonitrile containing 0.1% (v/v) trifluoroacetic acid, at a flow rate of 2.0 ml/min. The profiles A, B, C and D show the separation of fractions 3, 4, 6 and 7, respectively. The horizontal bars indicate the fractions collected for further studies.

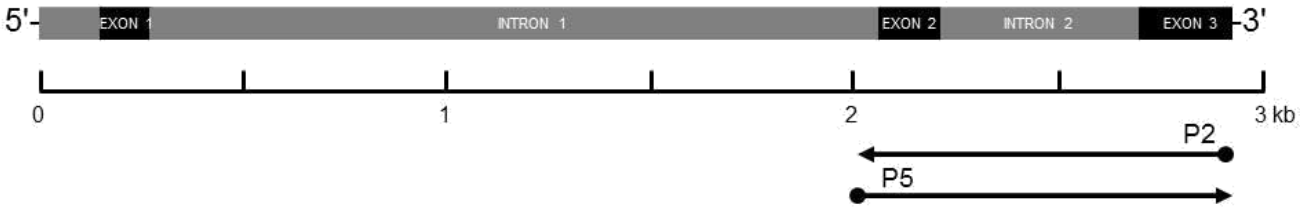

Supplementary Figure 2. Schematic drawing showing the genetic organization of the α-BgTx (A31 and V31) genes according to Chang et al. (1999) and approximate positions (dots) of the oligonucleotide primers P2 and P5.

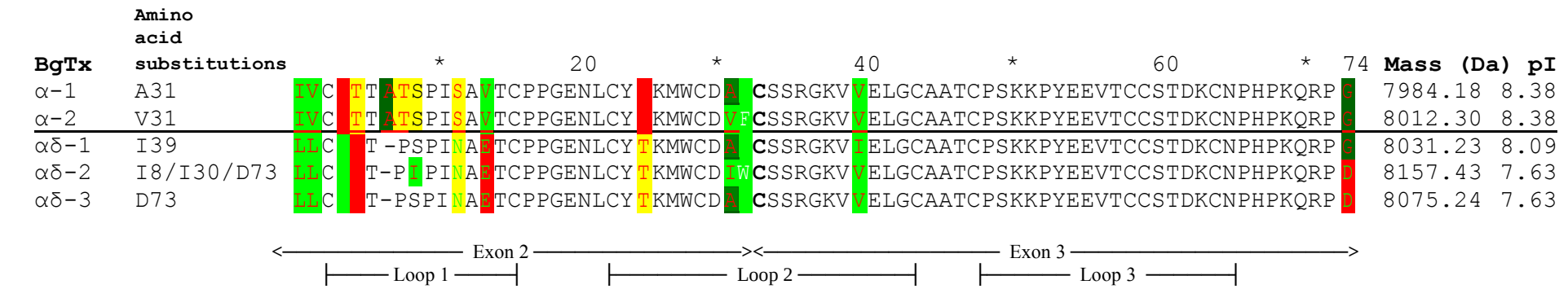

Supplementary Figure 3. Amino acid sequences, theoretical masses corrected for five disulfide bonds, and theoretical pIs of unique mature α-BgTx and αδ-BgTx polypeptides deduced from genomic DNAs. Variable residues shaded by the chemical property mode of Genedoc 2.6 using the programme's default settings. Residues interrupted by intron 2 appear in bold print. α-BgTx-1 and α-BgTx-2 (A31 and V31 isoforms, respectively) are from Chang et al. (1999). The numbers of amino acid replacements in αδ-BgTxs are given without taking into account the deletion in position 7.

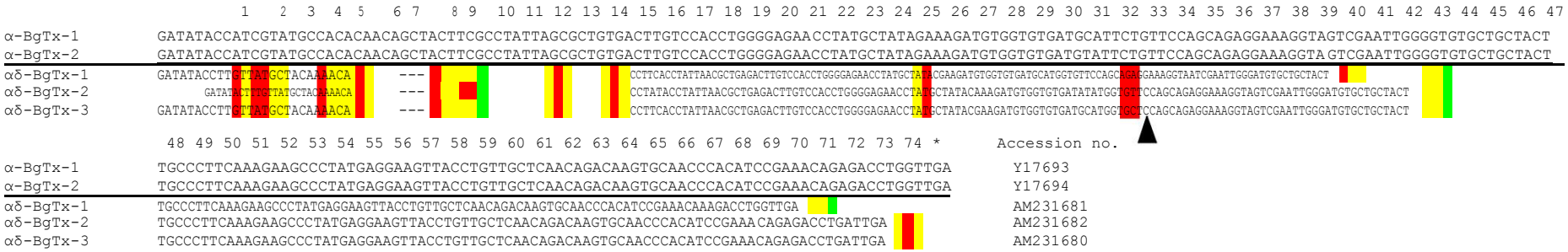

Supplementary Figure 4. Joined nucleotide sequences of exons 2 and 3 encoding unique α-BgTx and αδ-BgTx precursors. Toxin numbering is that of Fig. S3 Exon boundary indicated by triangle; 3'-non-coding nucleotides of exon 3 deleted. Numbers above sequences indicate the amino acid residues of mature α-BgTx. Unnumbered 5'-terminal nucleotides of exon 2 encode part of the signal peptide. Codons with substitutions relative to the α-BgTx-1 sequence are coloured; red and green highlight non-synonymous and synonymous substitutions, respectively; yellow, nucleotides that are invariant in these codons. α-BgTx-1 and α-BgTx-2 (A31 and V31 isoforms, respectively) are from Chang et al. (1999).

References

Chang, L.S., Lin, J., Chou, Y.C. and Hong E. (1997) Genomic structures of cardiotoxin 4 and cobrotoxin from *Naja naja atra* (Taiwan cobra). *Biochem. Biophys. Res. Commun* **239**, 756–762 https://doi.org/10.1006/bbrc.1997.7549

Chang, L.S., Lin, S.K., Huang, H.B. and Hsiao M. (1999) Genetic organization of α-bungarotoxins from *Bungarus multicinctus* (Taiwan banded krait): evidence showing that the production of α-bungarotoxin isotoxins is not derived from edited mRNAs. *Nucleic Acids Res.* **27**, 3970–3975 PMID:10497260

Kuch, U., Molles, B.E., Satoh, T., Chanhome, L., Samejima, Y. and Mebs, D. (2003) Identification of alpha-bungarotoxin (A31) as the major postsynaptic neurotoxin, and complete nucleotide identity of a genomic DNA of *Bungarus candidus* from Java with exons of the *Bungarus multicinctus* alpha-bungarotoxin (A31) gene. *Toxicon* **42**, 381–390 https://doi.org/10.1016/S0041-0101(03)00168-5

Nicholas, K. B., Nicholas, H. B., Jr. 2000. GeneDoc. Multiple sequence alignment editor and shading utility, version 2.6.001. Distributed by the author (www.psc.edu/biomed/genedoc).

Primer Name	Direction	Length (nt)	Sequence (5' to 3')	T_m (°C)	Reference
P2	H	24	GGATGGTCCTTGATGGATGAGAGC	67.11	Chang et al. (1999)
P5	L	25	GGGGAATGAGTATATACTTGTGTTT	59.66	Kuch et al. (2003)

Supplementary Table 1. Oligonucleotide primers used for PCR amplifications of αδ-BgTx encoding gene sequences.

The primer P2 of Chang et al. (1999) is based on the 3'-untranslated region of cobrotoxin and cardiotoxin genes (Fig. S1; Chang et al., 1997), and the primer P5 is designed to match a sequence upstream from exon 2 of the α-BgTx (A31) gene (Fig. S1; Kuch et al., 2003).